EFFECTS OF CHLORINE IN COAL ON BOILER SUPERHEATER/REHEATER CORROSION

M.-I.M. Chou and J.M. Lytle
Illinois State Geological Survey
Champaign, IL 61801

S. C. Kung
McDermott Technology Inc.
1562 Beeson St., Alliance, OH 44601

K.K. Ho
Illinois Clean Coal Institute
Carterville, IL 62918

Keywords: chlorine, coal, corrosion

Abstract
Many British studies have correlated superheater/reheater corrosion in pulverized coal boilers with the total chlorine (Cl) content in coals, which has led many US boiler manufacturers to set their maximum recommended Cl level at 0.3%. However, Cl-related boiler corrosion has not been reported by US utilities burning high-Cl Illinois coals. Other factors, such as boiler parameters, have been studied for their effect on corrosion rate. This study measured the rate of corrosion caused by two high-Cl coals (British and Illinois) and one low-Cl Illinois coal under identical pilot-scale combustion conditions for a duration which would give reliable comparisons. The results showed no correlation between coal Cl content and rate of corrosion, but showed a correlation between the rate of corrosion and the metal temperature used. These data could provide a basis for lifting the limit of burning high chlorine Illinois coals in the utility boilers.

Introduction
Many British studies have correlated accelerated fireside corrosion of heat exchanger tubes in utility boilers with the high-Cl content in coal (Raask, 1963; Reid, 1971; Meadowcroft and Manning, 1983). Their correlations implied that the corrosion rate of boiler tubes increased proportionally with increasing Cl concentration in the coal. Based on these correlations, US boiler manufacturers and utility operators consider coals containing more than 0.3% Cl to be potentially corrosive and have set guidelines on the Cl content (<0.3%) of coal to be used in their boilers. These guidelines were based primarily on extrapolation British coal data to predict the probable corrosion behavior of US coals. The guidelines on the Cl level have discouraged the burning of high-Cl Illinois Basin coals in utility boilers.

A survey conducted jointly by Electric Power Research Institute and Illinois Clean Coal Institute during 1992 (Doane et al., 1994; Wright et al., 1994) indicated that some US utilities have decades of experience burning high-Cl coals in pulverized coal (PC) fired boilers. Although fireside corrosion problems have been reported, none of them could be directly related to the presence of Cl in coal. This contradiction with published data suggested that the role of Cl in coal on boiler-tube corrosion was not fully understood. It is possible that the level of Cl in coal is not as harmful as predicted, or the corrosivity of high-Cl Illinois coal is less severe than that of British coal, or other coal properties such as sulfur and potentially volatile alkali metals in coals are possibly associated with boiler corrosion (Chou et al. 1998). The differences in boiler design and operation between US and UK utilities, such as boiler superheater/reheater temperatures, might also have attributed to this discrepancy.

This study focuses on how the corrosivity of a high-Cl Illinois coal compares with that of a British coal with a similar Cl content at superheater/reheater temperatures. Three pilot-scale combustion tests were conducted . The rates of corrosion caused by two high-Cl coals (British and Illinois) and a low-Cl baseline Illinois coal were measured under identical combustion conditions for a duration which would give a reliable comparison. The corrosion tests used Alloy 304SS which is a frequently used material at the hottest superheater section of both US and UK utility boilers. The corrosivity data from a temperature range including two specific metal temperatures, 1100°F and 1200°F were determined. The cooler metal temperature is common in the US boilers and the hotter temperature is common in the UK boilers.

Experimental
Coal samples - During sample acquisition, the available high-Cl British coals from the British Coal

Corporation Coal Research Establishment (CRE) coal sample bank were obtained for screening analysis (CRE, 1993). One of the coals obtained had a chlorine content (~0.4%) comparable to that of the high-Cl Illinois coal chosen. This British coal is also currently the most mined coal. A 20-ton lot of the British coal, therefore, was purchased from RJB Mining in Great Britain and shipped to the US for the combustion test. To form a basis for assessing the corrosion effect of the two high-Cl coals, a low-Cl Illinois coal was included in the combustion tests. Splits of the 20-ton lots of the three coals were analyzed for chlorine, sulfur, and ash content using the ASTM methods (1994).

Pilot scale combustion test - A refractory-lined, stoker-fired Fireside Corrosion Test Facility at McDermott Technologies, Inc. in Alliance, Ohio was used to burn the coal. A variable-speed screw feeder supplied the coal to the bottom of the stoker combustion chamber. A forced draft fan provided the primary air that entered the furnace through tuyers surrounding the burner. Penetrations right above the combustion chamber were used to accommodate the corrosion probes. Two sets of probes were used to approximate US and UK boiler tube wall temperatures. One set was regulated to include the temperature of 1200°F (649°C) which is common in UK boilers, and the other set was regulated to include the temperature of 1100°F (593°C) which is common in US boilers. A frequently used commercial alloy at the hottest superheater section of utility boilers was used to fabricate the corrosion probes. The ASTM designation of this alloy is SA213-T304 (304SS). The nominal composition of 304SS is given in Table 1. The essential features of the test matrix are given in Table 2.

High-temperature corrosion probe designation -Tube samples of the alloy in a dimension of 1" in outside diameter by 0.94" in length were fabricated and placed in series (Figure 1). The ends of each tube segment were shaped to extrude and concave chamfers at 10° and 45°, respectively. The chamfers allowed multiple segments to be assembled on the corrosion probe with an air-tight seal. A mechanical force was applied to the ends of the probes so that a tight fit could be achieved. Duplicate samples of the alloy were included in the corrosion probes. Type-K thermocouples were attached to one of the tube samples through the inner surface of the probes. The thermocouple junctions were positioned in EDM-drilled holes inside the samples facing the flue gas. Room-temperature compressed air was used to cool the corrosion probes and maintain the metal temperatures. Flow rate of the cooling air was regulated automatically by a controller that responded to the set points of the probe temperatures.

Corrosion rate measurements - The initial weight and initial outer diameter of each tube sample were measured. In addition, the wall thicknesses were carefully measured around the perimeter of each sample at eight points. The points were identified as 12:00, 1:30, 3:00, 4:30, 6:00, 7:30, 9:00, and 10:30 positions, with the 12:00 position being the leading edge facing the flue gas (Figure 2). After fireside corrosion exposure was completed, it was found that metal wastage on the inner surface of the tube samples were negligible, so only outside diameters of the tube samples were measured. All measurements were made in the middle section of the tube samples.

After the corrosion exposure, one of the duplicate samples was chemically cleaned. The chemical cleaning removed the coal ash deposit and scale formed on the sample surfaces during the exposure. After the cleaning, the final weight was again measured. Based on the total weight changes and initial surface areas, the average corrosion rates of the alloy were calculated. The wall thicknesses of the chemically cleaned samples were also measured at the same positions mentioned above. As a result, the corrosion wastage of the tube samples could be determined, which were subsequently used to calculate the local corrosion rates. The corrosion rates for the two high-Cl coals were extrapolated from the 1000-hour test result and reported as mils per year (mpy). Because of equipment difficulty during the low-Cl coal test, the sample was only combusted for 813 hours. The data, however, were again extrapolated and reported in mpy for comparisons with the other coals.

Cross sectional examination - A cross-section was prepared metallograpically from one of the alloy samples after the corrosion exposure. The sample was mounted in Bakelite, cut, and polished dry to preserve any water-soluble compounds that might exist on the alloy surfaces. The ash and scale layers of the sample from each test were examined under an optical microscope and a scanning electron microscope (SEM) equipped with energy dispersive X-ray (EDX) analytical capability. The remaining metal thicknesses of the samples were also determined using a Nikon Microscope at the eight positions as described before.

Results and Discussion

Chemical composition of the three coal samples - Splits of the 20-ton lots of the three coals were analyzed for chlorine, sulfur, and ash content (Table 3). The two high-Cl coals contained medium-

sulfur contents; whereas, the low-Cl Illinois coal contained high-sulfur content. Also, the as-shipped Illinois high-Cl coals had much less ash than did the British high-Cl coal.

Pilot Scale Combustion - Rate of Corrosion

Three long-term, pilot-scale combustion tests were conducted using SA213-T304 (304SS) to evaluate boiler corrosion produced at two specific boiler wall temperatures. The corrosion rate was most pronounced at the 1:30, 3:00, 9:00, and 10:30 positions; in other words 30 to 90° from the leading edge (Figure 2). These measurements were extrapolated to the amount of corrosion in one year or mils per year (mpy).

High-Cl Illinois coal - In general, the corrosion rates at the leading edge (12:00 position) were less than those measured at 30 to 90° away from the leading edge. For example, the corrosion rate of 304SS at 1100°F at the 12:00 position was approximately 40 mpy (not shown), while the greatest corrosion rate between 30 to 90° positions was greater than 100 mpy (shown in Figure 3). Such variation was consistent with the general observation of superheater corrosion in the field. The changes for the corrosion rate with respect to metal temperature at the positions between 30 to 90° are shown in Figure 3. The corrosion rate of 304SS within the temperature range analyzed appeared to show an earlier stage of a bell-shape relationship. It showed increases with increasing metal temperature; and the increases in the corrosion rate were quite significant. For example, the corrosion rate was approximately 120 mpy at 1100°F, and about 260 mpy at 1200°F.

High-Cl British coal - Similarly, the corrosion occurring on the probes at the 30 to 90° locations was more severe than that at the leading edge. The changes of corrosion rate at the positions between 30 to 90° locations with respect to increasing metal temperature are shown in Figure 4. The corrosion rate, similar to what was seen in the test for the high-Cl Illinois coal, increased consistently with increasing metal temperature; and the increases in the corrosion rate were quite significant. The corrosion rate was about 190 mpy at 1100°F, and about 267 mpy at 1200°F

Low-Cl Illinois coal - As usual, the corrosion occurring on the probes at the 30 to 90° locations was more severe than at the leading edge. The changes of corrosion rate between the 30 to 90° positions with respect to increasing metal temperature are shown in Figure 5. Similar to the tests of high-Cl coals, the corrosion rate increased consistently with increasing metal temperature, and the increases in the corrosion rate were quite significant. The corrosion rate was about 120 mpy at 1100°F; and about 250 mpy at 1200°F.

In general, the data showed no correlation between the rate of corrosion and the chlorine content in coal. The results showed a correlation between the rate of corrosion and the metal temperature used. Within the range of the metal temperatures used, a greater corrosion rate was observed at the higher metal temperature. In addition, the corrosion rates observed for the British coal appeared to be slightly greater than those of the two Illinois coals.

Summary and Conclusions

The results of pilot-scale combustion tests showed no correlation between the coal Cl content and rate of corrosion, but showed a correlation of the rate of corrosion with the metal temperature used. The corrosion rate was increased with an increase in the metal temperature during the combustion for all three coals. These data suggested that the different field history of the corrosivity caused by burning high-Cl Illinois coal and high-Cl British coal might have been the result of different superheater/reheater metal temperatures used in the US and UK utility boilers. These data could provide a basis for lifting the limit of burning high chlorine Illinois coals in the utility boilers

Acknowledgment & disclaimer

This study was supported, in part, by grants made possible by U.S. Department of Energy (DOE) Cooperative Agreement Number DEFC22-PC92521, the Illinois Coal Development Board (ICDB), and the Illinois Clean Coal Institute (ICCI). Neither the authors nor any of the subcontractors, nor the U.S. DOE, ISGS, ICDB, ICCI, nor any person acting on behalf of either assumes any liabilities with respect to the use of, or damages resulting from the use of, any information disclosed in this paper. The authors wish to thank Dr. Murray Abbott of CONSOL Inc. Dr. Nigel Paterson of the British Coal Corporation, and Ms. Lisa Duffy and Mr. Charles Smith of Freeman Energy Co. for providing coal samples.

References

ASTM Book of Standards, Vol 5.05 Gaseous Fuels; Coal and Coke, D2361, D3177, D3173, D3174 and D3685, American Standard Testing Materials, 1994.

Chou, M.-I., J.M. Lytle, J.A. Bruinius, S.M. Kung, and K.K. Ho. 1998. Effects of Chlorine in Coal on Boiler Corrosion. Final Report to the Illinois Coal Development Board, Illinois Clean Coal Institute. September1, 1996 - March 31, 1998.

CRE, The CRE Sample Bank: Users Handbook, Gloucestershire, UK, 1993.

Doane E.P., J.A.L. Campbell, and M.F. Abbott, Combustion of High-Chlorine Illinois Basin Coals in Utility Boilers, Proceedings: The Effect of Coal Quality on Power Plants, Fourth International Conference, EPRI, August 1994.

Meadowcroft D.B.and M.I. Manning, Corrosion Resistant Materials for Coal Corrosion Systems, Applied Science Publishers LTD, Essex England, 1983.

Raask, E. in the Mechanism of corrosion by fuel impurities, Butterworths, London, 1963, pp.145-154.

Reid, W.T., External Corrosion and Deposits in Boilers and Gas Turbines, American Elsevier Publishing Company, Inc., New York, pp.138-142, 1971.

Wright, I.G., A.K. Mehta, and K.K. Ho, Survey of the Effects of Coal Chlorine Levels on Fireside Corrosion in Pulverized Coal-Fired Boiler, in postprints of second annual EPRI conference on Effects of Coal Quality on Power Plants, August 17-19, 1994.

Table 1. Partial composition of 304SS superheater alloy in wt%

Element	C	Mn	P	S	Si	Ni	Cr
%	≤0.08	≤2.0	≤0.04	≤0.03	≤0.75	8-11	18-20

The balance of the alloy is Fe.

Table 2. Test matrix for pilot scale stoker boiler combustion

Test	Coal Sample	Metal temperature*
A	High-Cl IL coal	1100°F
B	High-Cl IL coal	1200°F
C	High-Cl British Coal	1100°F
D	High-Cl British Coal	1200°F
E	Low-Cl IL Coal	1100°F
F	Low-Cl IL Coal	1200°F

* Actually, the rate of corrosions were measured for four temperatures within a range from1000 to 1200°F.

Table 3. Total chlorine, total sulfur, and ash content of the three coals.

wt % dry coal basis	High-Cl IL Coal	High-Cl British Coal	Low-Cl IL Coal
Total Chlorine	0.44	0.46	0.14
Total Sulfur	1.22	1.32	4.48
Ash	7.90	23.56	9.38

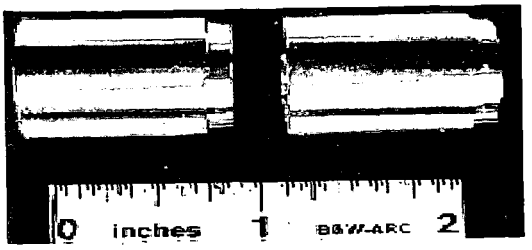

Figure 1: Arrangement of the chamfered tube segments on the corrosion probe

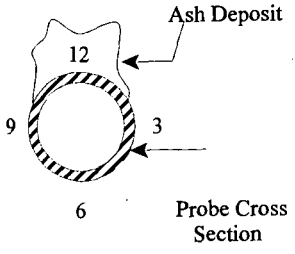

Figure 2. Illustration of the probe cross section, the leading edge (12:00 position), and the 30° to 90° area away from the leading edge for corrosion rate measurement

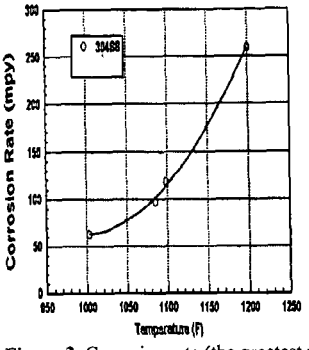

Figure 3. Corrosion rate (the greatest value) versus temperature at the positions between 30° and 90° for the test burning the high-Cl Illinois coal.

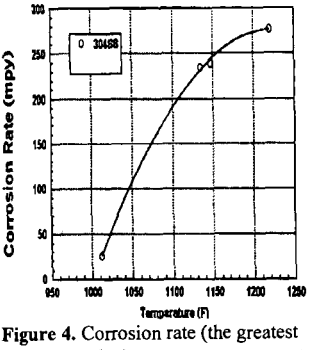

Figure 4. Corrosion rate (the greatest value) versus temperature at the positions between 30° and 90° for the test burning the high-Cl British coal.

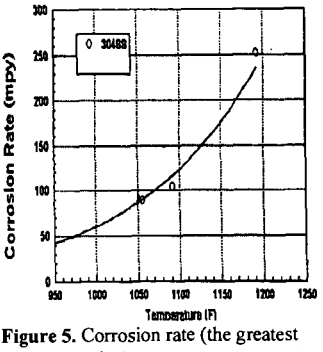

Figure 5. Corrosion rate (the greatest value) versus temperature at the positions between 30° and 90° for the test burning the low-Cl Illinois coal.

QUANTITATIVE EVALUATION OF SULFUR TYPES IN MIDDLE DISTILLATES

Y. Briker, P. Rahimi, A. Iacchelli, Z. Ring and C. Fairbridge
National Centre for Upgrading Technology, 1Oil Patch Drive,Suite A202, DEVON, Alberta T9G 1A8, Canada
R. Malhotra
SRI International, 333 Ravanswood Avenue, Menlo Park, CA 94025

KEYWORDS: sulphur determination in fuels, field ionization mass spectrometry, hydrocarbon type analysis

ABSTRACT

The utilization of fossil fuels in the transportation sector is changing. Due to increasing environmental constrains it is anticipated that changes in transportation fuel specification will be required. It will be necessary to improve diesel fuel quality to address the problems of emission from diesel powered vehicles. A trend in the transportation fuel production indicates an increase of the proportion of diesel fuel produced from oil sands and heavy crude oil. The relatively poor ignition quality of this middle distillate puts pressure on the petroleum industry to produce fuel that is more environmentally clean and yet economically feasible. In the future, knowing which of fuels' physical and chemical properties influence engine exhaust emissions will become very important. Currently, there are several mass spectrometry techniques that can determine the hydrocarbon type composition of diesel fuels. This paper will discuss the results of hydrocarbon type analyses obtained for middle distillate sample by using HVLREI GC-MSD (high voltage low resolution electron impact mass spectrometry) and GC-FIMS (Field Ionization Mass Spectrometry). Comparison of aromatic sulfur types, such as di- and benzothiophenes, calculated by mass spectrometry methods and by GC-FID/SCD (Sulfur Chemiluminescent Detector) will be discussed.

INTRODUCTION

There are few standardized methods available based on high voltage low resolution electron impact mass spectrometry to perform detailed analyses of complex petroleum mixtures. For fractions boiling in the naphtha range, the ASTM 2789 method is used. For hydrocarbon distillates boiling above the naphtha range, prior chromatographic separation is usually required in order to avoid interference between saturate and aromatic types. The saturate fraction can be analyzed by the ASTM 2786 methods and the aromatic fraction, by the ASTM 3239 method for petroleum fractions boiling within the range from 205 to 540 °C. For fractions boiling within the diesel range (177 to 343°C),the ASTM 2425 method is applied. The Robinson method offers a one-step analysis that does not require the separation into saturate and aromatic fractions. The method, developed by C. J. Robinson in 1971(1), covers the full boiling range and resolves up to 4 saturate and 21 aromatic compound types including 3 thiophenoaromatic types (assuming no olefins are present in the sample).

There is also a GC-FIMS method that identifies the composition of liquid fuel by compound type (z-values) and molecular size (2). The method, developed at SRI, is based on replacing the electron-impact ionizer of an HP GC-MSD system with the SRI volcano-style field ionizer. For most compounds, field ionization produces only the molecular ion. Analysis by FIMS expresses the data as z-series tables giving the composition by compound type (z-values) and molecular size (number of carbon atoms).

This work is a continuation of the GC-FIMS application for compositional analysis of transportation fuels (3). We analyzed light cycle oil (LCO) by GC-MSD and by GC-FIMS for hydrocarbon type composition and found some pronounced differences, especially in the saturate types. The distribution of aromatic types was identical. In order to evaluate the methods, we analyzed one of the samples by GC/FID/SCD(sulfur chemiluminescence detector) in order to quantify the thiophenoaromatic types present in the sample. We compared these results with those obtained by mass spectrometry methods.

EXPERIMENTAL

Initially, the fuel sample was analyzed by GC-MSD and the hydrocarbon types were calculated using the Robinson method. The sample was then separated into saturate, aromatic and polar fractions using a liquid chromatographic procedure, which was a modified ASTM D2007 method (4). The saturate and aromatic fractions were analyzed separately by both, GC-MSD and by GC-FIMS. The aromatic fraction composition was calculated by ASTM D3239, and the saturate fraction composition was calculated by ASTM D2786. The computer programs for calculation of hydrocarbon types were written by R. Teeter (5) based on modification of the original methods and supplied by PSMASPEC, USA.

For GC-MSD runs, a Hewlett Packard GC-MS with HP 5972 MSD, HP 7673 GC/SFC injector and HP 5890 GC was used. The column was a 30m x 0.25mm x 0.25μm High

Resolution GC Column J122-5532 DB-5MS. The oven was held at 35°C for 3 min and was then heated at 10°C/min to 280°C. The MSD temperature was 280°C. The cool on-column injection technique was employed with helium as the carrier gas at a constant flow rate of 1.2 ml/min.

For the GC-FIMS runs, a 30-m x 0.25mm x 0.25µm HP1-MS non-bonded column was used. The injection (0.2µl; 19:1 split) was made with the oven at 45°C. The oven was heated at 17°C/min to 300°C. Sulphur determination was performed using Hewlett Packard gas chromatograph HP6890 series equipped with cool on-column injector and nonaliter adapter, FID/SCD detector (Sulphur Chemiluminescence Detector) SIEVERS 355. The HP 19091Z-213, HP-1 Methyl siloxane (30.0m x 320.00µm x 1.00µm) column with the injection volume of 0.5µl was used. The total sulphur content was calculated by using the response factor determined from running the sulphur standard with the known sulphur concentration. For aromatic sulfur speciation, the standards benzothiophene and dibenzothiophene were analyzed. Knowing the retention time for both compounds, the baseline integration was performed separately for benzothiophenes and dibenzothiophenes on the sample chromatogram. Then, each of the sulfur groups was calculated knowing the response factor and assuming the average molecular weight 190 Da for benzothiophenes and 220 Da for dibenzothiophenes. The calculated result was confirmed with the result obtained by using the standard method for sulfur determination such as: ASTM D4294 (Sulfur in Petroleum Products by Energy-Dispersive X-Ray Fluorescence Spectroscopy).

RESULTS AND DISCUSSION

HYDROCARBON TYPES

The GC-MSD and GC-FIMS results are presented in Table1. The results for separated fractions are presented together with the Robinson results for the total sample. The hydrocarbon type composition of fuels analyzed by GC-FIMS is usually presented as a z-series. All the numbers in a z-table (Table 2) are given as sums of the weight fractions from C_1 to C_{20} for z-numbers from -2 to -14. The elemental formula of any hydrocarbon can be generally expressed as C_nH_{2n+z}, where z is a measure of the unsaturation index. All acyclic alkanes have the general formula of C_nH_{2n+2} (i.e., z-value of +2), and monocyclic alkanes have the general formula of C_nH_{2n} (i.e., a z-value of 0). The z-value decreases by 2 for every degree of unsaturation (ring or double bond). Since the fractions were analyzed separately, it was possible to identify all the saturate types and some of the aromatic types without any interference.

In Table 1, each saturate type in the GC-FIMS column corresponds to a z-series number given in Table 2 for the saturate fraction. It is quite noticeable that the saturate region mainly covers the intensities in z series from +2 to –4, that is from paraffins to tricyclic alkanes. The aromatic region covers mainly the intensities in z series from –6 to –14 corresponding to alkylbenzenes up to naphthocycloalkanes. Some of the peaks detected with z <-6 in the saturate fraction could be attributed to some aromatic impurities due an incomplete separation. The numbers in Table 1 suggest that in this case those impurities are negligible. For the aromatic fraction, the masses detected in the saturate region are also minor and could be due to a small amount of saturates, such as tricycloalkanes, that are left behind after saturate separation and later coeluted with the aromatics.

In Table 1, there are three columns for the results from GC-FIMS analysis. The first column is a direct translation of a z-table into hydrocarbon types. First, comparison of the aromatic types obtained by GC-MSD and FIMS suggested that there was a difference in the polyaromatic types. FIMS showed results about 10% higher for the total mono- and diaromatics. The difference in alkylbenzenes was 11%, in naphthalenes, 17%. Tri- and tetraaromatics were not calculated by FIMS, while they were 9.0% and 2.9% by ASTM D3239. These differences could be explained by the fact that because of the limited number of samples analyzed by GC-FIMS, the response factors for various series have not yet been optimized. Furthermore, at this stage of development, FIMS only calculates the hydrocarbon types for lighter material.

However, by analyzing the SICs (single ion chromatograms) from the GC-FIMS analysis of LCO, compounds such as fluorenes (z-16), phenanthrenes (z-18), phenanthrocycloalkanes (z-20) and pyrenes (z-22) were found in the spectra. In order to avoid a discrepancy between the actual spectra and the results of a z-table, it was assumed that the amount of phenanthrenes, fluorenes and pyrenes calculated by FIMS would be very close to the ones calculated by other MS methods. According to data in Table 1, there was no significant difference between the aromatic types obtained by ASTM D3239 and the Robinson method. The aromatic compounds tend not to fragment too much when analyzed by both techniques and there is reason to believe that the analysis by FIMS would produce a similar distribution. The amount assumed for phenanthrenes was 9.0%, for fluorenes , 5.0%, and for pyrenes, 3.0% (average from ASTM3239 and Robinson results). Recalculated results are presented in the second column of FIMS analysis (Table 1). Now the comparison was much better with the results from other GC-MS methods with the exception of alkylbenzenes and naphthalenes. These are the groups that overlap with the aromatic sulfur types.

In order to compare two different MS methods, we had to compare results for all hydrocarbon types. When the Robinson and ASTM 2786 methods were compared, the total

amount of cycloparaffins was in a good agreement, however, there were differences within the cycloparaffinic types and between straight chain paraffins. The values for normal paraffins and polycycloparaffins calculated by ASTM 2786 were higher than the corresponding values calculated by the Robinson method while the order was reversed for monocycloparaffins. For samples where the saturates content is high and cycloparaffin content is high, these differences could be much more profound. There is a method, INT 101 (6), that overcomes the discrepancies of the Robinson method, however it still does not answer the question of true saturates distributions. Comparison of saturates distribution measured by the GC-FIMS and GC-MSD also could not answer this question.

If field ionization produced only the molecular ions, then it could be assumed that the results obtained by GC-FIMS would reflect the true distributions. Consequently, the results in Table 1, obtained by the electron impact GC-MSD, especially for the cycloparaffins, would be greatly underestimated. However, at this point the results obtained by FIMS for the saturate fraction do not quite reflect the compound distribution. The isoparaffins tend to fragment and do not produce the molecular ion. They can not be accounted for in the calculation and therefore lower the amount of the calculated total paraffins. It will be our future task to determine the proper response factors for various paraffin mixtures and adjust the calculation. At this point the methods could be evaluated based on aromatics distribution. We looked particularly at the aromatic sulfur distribution and compared it with the results determined by another method rather then mass spectrometry.

As mentioned before, the aromatics distributions for the sample were identical except for the overlapping species in FIMS results. The numbers with the asterisk (Table 1) present the sums of intensities for a particular z-series that have interference within the series, such as alkylbenzenes with benzothiophenes and naphthalenes with dibenzothiophenes. We were able to calculate the values for benzothiophenes and dibenzothiophenes. The calculation was performed by setting the separate time windows for the sulfur and the hydrocarbon types. It was possible since the two species were separated by GC prior to being analyzed by FIMS.

The nominal mass of dibenzothiophene is 184 Da, which is the same as that of a C_4-naphthalene. Figure 1 shows the selected ion chromatograms (SICs) for m/z 184, 198, 212, 226, 240 and 254 extracted from the TIC of MD2-aromatics. The C_4-naphthalenes (m/z 184) elute between 9.4 and 10.6 min. The cluster of peaks due to C_4-naphthalenes is followed by a strong peak at 10.8 min., which is due to dibenzothiophene. The control run of dibenzothiophene is shown in Figure 2. The SIC of mass 198 in Figure 1 shows a similar pattern as that found for m/z 184. Here, the alkylnaphthalenes are between 9.2 and 11.2 min., and the isomeric methyldibenzothiophenes are between 11.3 and 12.4 min. The pattern is repeated for the SICs of other masses up to mass 268. Integration was performed for the dibenzothiophene portion of the SIC for every extracted mass. The integrated area was related to the total area of the SIC. The ratio then was multiplied by a corresponding mass percent taken from a z-table in order to calculate the dibenzothiophene portion (assuming the response factors being the same for both compound types). The same exercise was performed for benzothiophenes (the SICs for m/z 134, 148, 162, 176, 190 and 204 were extracted). The integration was done for benzothiophenes with m/z up to 232.

LCO was analyzed also by another technique, GC/SCD (gas chromatograph/ sulfur chemiluminescence detector). The GC/SCD chromatogram of this run is presented in Figure 3(a). The chromatograms of benzothiophene (retention time 19.520 min.) and dibenzothiophene (retention time 32.686 min.) standards are presented in Figures 3(b) and 3(c) respectively. The total sulfur was calculated using the total area and the factor as was explained earlier. The sulfur obtained by this method was 1.38wt.%. This number was verified by the ASTM 4294 method (Dispersive x-Ray Fluorescence Spectroscopy) which reported sulfur of 1.45wt.%. Knowing the retention time for benzothiophene and dibenzothiophene, part of the chromatogram was integrated between 19.52 and the beginning of peak at 32.686 min. for benzothiophenes, and between start of peak at 32.686min to the end for dibenzothiophenes. The calculation was performed according to a procedure described above. The results of sulfur determination are summerized in Table 3.

Total sulfur determined by GC/SCD was in a good agreement with the result from ASTM 4294. The result obtained by the GC- FIMS was the closest to the SCD result, especially in terms of distribution between di- and benzothiophenes. This comparison favors the GC-FIMS method for calculation of other hydrocarbon types in fuels with a high degree of accuracy provided that the response factors for the paraffins would be adjusted.

CONCLUSION

The results presented in this paper demonstrate the ability of various GC-MS methods to provide rapid and detailed group-type analysis of middle distillates. Analysis of data from each method suggests a discrepancy, particularly for saturates distribution, between the Robinson method for unseparated sample and between ASTM D2786 and ASTM D3239 for separated fractions. The difference was even greater when these results were compared with GC-FIMS

results. Comparison of di- and benzothiophenes content in one of the samples calculated by different methods indicates that analysis by GC-FIMS may offer more reliable distribution of hydrocarbon types compared to the other two methods, provided that the results would be corrected for the isoparaffins fragmentation. The GC-FIMS combination allowed the overlapping species in the same z-series to be separated by time and thus accurately calculated. By creating separate time windows for the GC-separated species and determining their response factors it could be possible to analyze the samples having a full boiling range without prior separation.

REFERENCES

1. C. J. Robinson, *Anal. Chem.*, **1971**, 43, 1425.
2. R. Malhotra, M. J. Coggiola, S.E. Young, C.A. Spindt, "*Analysis of Transportation Fuels", AM Chem. Soc., Div. Petr. Chem., Preprints*, **1996**, 41(4), 652.
3. R. Malhotra, M. J. Coggiola, S.E. Young, S. Hsu Chang, J.Dechert, Exxon, P. M. Rahimi, Y. Briker, "*Rapid Detailed Analysis of Diesel Fuels by GC-FIMS*", AM Chem. Soc., Div. Petr. Chem., Preprints, **1998**.
4. Y, Briker, P.Rahimi, N.Mclean, A. Iacccelli, Z. Ring, and C. Fairbridge, "*Process Modeling: Development of a Procedure for the Distribution of GC-MS Hydrocarbon Type Characterization by Boiling Point*", NCUT Report 98-09.
5. Richard M. Teeter, "*Software for calculation of hydrocarbon types*", PCMASPEC, 1925 Cactus Court, #2, Walnut Creek, CA 94595-2505, USA.
6. C. Pachego and M. Hazos, INTEVEP, S.A., "*Aromatic and Saturate Analysis by Low Resolution Mass Spectrometry*", AM Chem. Soc., Div. Petr. Chem., Preprints, August 23-28, 1992.

Table 1 – Comparison of hydrocarbon type analyses results for Light Cycle Oil by different GC-MS methods

Hydrocarbon CnH2n+Z	Z No.	Robinson Total	ASTM 2786 Saturates	ASTM 3239 Aromat.	GC-FIMS Saturates	GC-FIMS Aromat.1	GC-FIMS Aromat.2	GC-FIMS Aromat.3
SATURATES		**21.90**	**22.70**		**22.70**			
Paraffins	2	11.90	12.40		5.96			
Cycloparaffins		**10.00**	**10.30**		**16.74**			
Monocycloparaffins	0	6.40	4.10		7.92			
Dicycloparaffins	-2	3.60	2.50		1.76			
Polycycloparaffins	-4	0.00	3.70		7.06			
AROMATICS		**78.10**		**73.70**		**73.70**	**73.70**	**73.70**
Monoaromatics		**21.50**		**20.40**		**29.70***	**22.90***	**19.60**
Alkylbenzenes	-6	9.50		8.60		21.10*	16.20*	12.90
Benzocycloalkanes	-8	9.70		9.60		7.10	5.50	5.50
Benzodicycloalkanes	-10	2.30		2.20		1.50	1.20	1.20
Diaromatics		**35.20**		**33.40**		**44.00**	**38.80***	**32.30**
Naphthalenes	-12	21.20		21.30		38.80*	29.80*	23.30
Naphthocycloalkanes	-14	7.60		6.80		5.20	4.00	4.00
Fluorenes	-16	6.30		5.30		0.00	5.00	5.00
Triaromatics		**10.70**		**9.00**		**0.00**	**9.00**	**9.00**
Phenanthrenes	-18	9.10		7.80		0.00	7.80	7.80
Phenanthrocycloalkanes	-20	1.60		1.20		0.00	1.20	1.20
Tetraaromatics		**3.30**		**2.90**		**0.00**	**3.00**	**3.00**
Pyrenes/Benzofluorenes	-22	2.70		2.60		0.00	3.00	3.00
Chrysenes	-24	0.50		0.30		0.00	0.00	0.00
Pentaaromatics		**0.00**		**0.20**		**0.00**	**0.00**	**0.00**
Chrysocycloalkanes	-26	0.00		0.20		0.00	0.00	0.00
Benzpyrenes/Perylenes	-28	0.00		0.00		0.00	0.00	0.00
Dibenzanthracenes	-30	0.00		0.00		0.00	0.00	0.00
Unidentified		**0.00**		**0.00**		**0.00**	**0.00**	**0.00**
CnH2n-32/CnH2n-46	-32	0.00		0.00		0.00	0.00	0.00
CnH2n-36/CnH2n-26S	-36	0.00		0.00		0.00	0.00	0.00
CnH2n-38/CnH2n-28S	-38	0.00		0.00		0.00	0.00	0.00
CnH2n-42/CnH2n-32S	-42	0.00		0.00		0.00	0.00	0.00
CnH2n-44/CnH2n-34S	-44	0.00		0.00		0.00	0.00	0.00
Aromatic Sulfur		**7.50**		**7.80**		**0.00**	**0.00**	**9.80**
Benzothiophenes	-10S	3.40		3.60		0.00	0.00	3.30
Dibenzothiophenes	-16S	3.90		4.00		0.00	0.00	6.50
Benzonaphthothiophenes	-22S	0.20		0.20		0.00	0.00	0.00

Arom.1- Original data from z-table
Arom.2- Data adjusted for polyaromatics
Arom.3- Data adjusted for aromatic sulfur

Table 2 - FIMS results for saturate and aromatic fractions of LCO by z-series

Sample ID	2	0	-2	-4	-6	-8	-10	-12	-14	
Aromatics(%of Ar.)	0.02	0.08	0.05	0.12	28.65	9.61	2.03	52.72	6.72	100.00
Aromatics(%of Total)	0.01	0.05	0.04	0.09	21.10	7.07	1.50	38.84	5.00	73.70
Aromatics(%of Ar.)*	0.01	0.06	0.04	0.09	22.06	7.40	1.57	40.60	5.17	77.00
Aromatics(%of Total)*	0.01	0.03	0.03	0.06	16.25	5.45	1.16	29.91	3.80	56.70
Saturates(%of Sat.)	26.28	34.92	7.82	24.04	0.42	2.89	3.34	0.35	0.16	100.24
Saturates(%of Total)	5.96	7.92	1.76	5.45	0.10	0.64	0.75	0.08	0.04	22.70

* - Results are recalculated for the presence of fluorenes, phenanthrenes and pyrenes

Table 3 – Aromatic sulfur types determined by different methods

Aromatic sulfur types Wt.% of total	ASTM 4294	GC-SCD	GC-FIMS	GC-MS ASTM D3239	GC-MS Robinson
Benzothiophenes	-	2.7	3.3	3.6	3.4
Dibenzothiophenes	-	6.0	6.5	4.0	3.9
Naphthobenzothiophenes	-	N/D	N/D	0.2	0.2
Total aromatic sulfur	-	8.7	9.8	7.8	7.5
Total sulfur	1.45	1.38	1.50	1.19	1.14

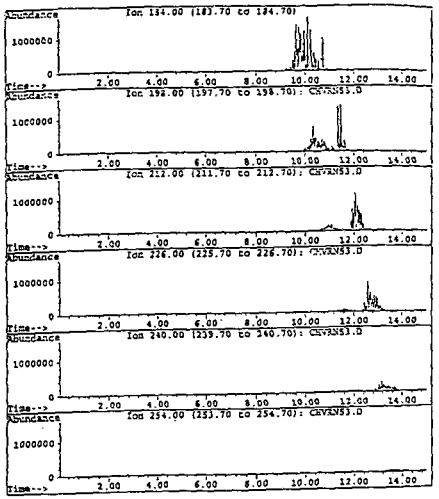

Figure 1. Selected Ion Chromatogram of m/z 184,198,212,226,240,254 Extracted from GC-FIMS analysis of LCO

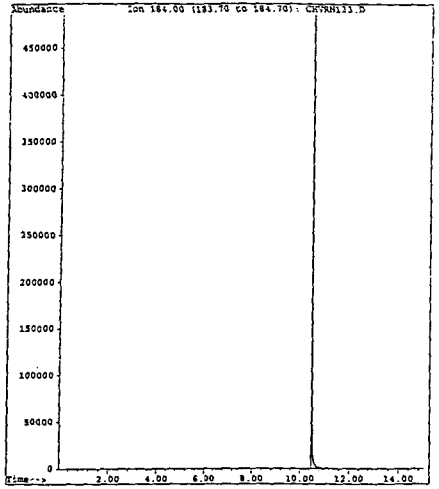

Figure 2. Selected Ion Chromatogram of m/z 184 extracted from GC-FIMS Analysis of dibenzothiophene

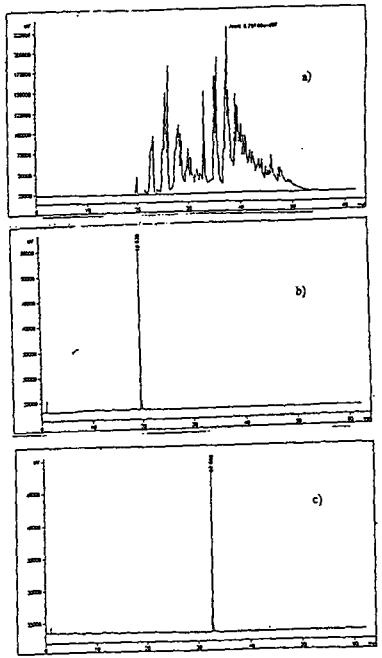

Figure 3. GC-FID/SCD chromatogram of LCO
a) GC-FID/SCD chromatogram of the total sample
b) GC-FID/SCD chromatogram of benzothiophene
c) GC-FID/SCD chromatogram of dibenzothiophene

BENCH SCALE CO-PYROLYSIS OF A LOW RANK COAL AND A PETROLEUM RESIDUE

I.Suelves, R.Moliner and M.J.Lázaro
Instituto de Carboquímica (CSIC). María de Luna, 12. 50015 Zaragoza (Spain)

INTRODUCTION

During coal pyrolysis, both degradation processes that create free radicals and crosslinking reactions, happen simultaneously. To increase the liquid yields obtained from coal pyrolysis radical stabilisation should be promoted and crosslinking reactions should be decreased[1-3]. However, coal hydrogen content is not high enough to promote this radical stabilisation and so that, hydrogen should be provided from other sources. One of the most promising ways of increasing the hydrogen content is provide it from hydrocarbon materials, specially hydrocarbon wastes that can be co-pyrolyzed with coal[4-7]. This way two benefits are expected: first coal may enhance the conversion of the hydrocarbon material and beside this the presence of the waste would improve the quality of the products obtained from coal. Petroleum residue is a very interesting material that observes the main characteristics needed to be used in this type of processes: hydrogen content, aliphatic nature, etc. However, there are few references in literature on this subject because the most important works on co-utilization of coal and petroleum residues are related with catalytic coprocessing reactions, using high hydrogen pressures. In our previous works at analytical scale we have shown that there is a synergetic effect for the production of some interesting compounds like light olefins and BTX when coal and petroleum residue are co-pyrolyzed[8,9]. Therefore at this scale, secondary reaetions were disfavoured and there was no possibility of stabilising mass balances or evaluating the influence of co-pyrolysis on char formation. For that reasons, the main objectives of this work are: (i) to evaluate the interactions between coal and petroleum residue during co-pyrolysis at bench scale and (ii) to study the influence of the experimental conditions on char formation.

EXPERIMENTAL

Different experimental series were carried out, each of them dedicated to the study of the influence of temperature, pressure and petroleum residue mass ratio on the mixture behaviour. Temperatures used were 600, 650 and 700ºC; pressures, 0.1, 0.5 and 1MPa and mass ratio (Coal/PR) 70/30 and 50/50.

Materials

Samca coal (Teruel, Spain) and a petroleum vacuum residue (PR) have been used in this work. Samca is a subbituminous coal with high volatile content and with high sulphur and oxygen content. The petroleum residue proceeds from the distillation of different crudes and has been submitted by REPSOL (Puertollano, Spain). The main characteristics of these materials have been described in our previous works [8,9].

Experimental installation

Bench scale pyrolysis unit used in this work has been shown elsewhere[10]. In summary it consists of an oven heated reactor with two different parts; the bottom of the reactor, where pyrolysis happens, is filled with a ceramic rings bed. The sample is feeded from the upper part and falls into the reactor by gravity. When the sample is introduced, the reactor has reached the pressure and temperature conditions of the pyrolysis run. Pyrolysis products are recovered from the bottom of the reactor sweeped by a nitrogen stream. They are cooled in a Peltier effect cooler. Liquids are collected in a liquid-cyclone and gases are collected in a gas sampling bag which volume is measured after each run.

Sample preparation

First coal and PR were pyrolyzed alone and then as a mixture. Preparation of the mixtures was as follows: PR was first solved in THF and then coal was added. The mixtures were subsequently sonicated. After 15 minutes, THF was evaporated by heating under vacuum. The dried samples were grounded to <0.2 mm. A cryogenic grounding technique was used in order to increase the grindibility of the sample and to improve the homogeneity of the mixtures. Samples of around 10g were used in each run

Analytical Methods

The ponderal yields of char and liquids were determined by direct weight whereas gas global-yields were calculated from the sum of the individual yields of each of the components obtained by gas-chromatography. A run was considered as a valid one if the ponderal yield sum of all recovered products was higher than 95%. Global results were normalised to 100% in order to facilitate comparison between runs.

Gases were analysed by gas chromatography using three separate analytical methods: a packed column of Molecularsieve 13X with nitrogen as carrier gas and TCD detection for hydrogen; two packed columns: Molecularsieve 13X and Porapak with helium as carrier and TCD

detection for permanent gases; an alumina capillar column with helium as carrier and FID detection for C_1-C_6 hydrocarbons. Hydrocarbons chromatographied between n-pentane and n-hexane were accounted for together as C_5. In the same way, compounds chromatographied between n-hexane and benzene were accounted for as C_6.Quantification of gas components was carried out by means of standard gas mixtures.

Liquids were formed by the organic phase, tar and water. The separation of tar and water was very difficult, so that they were weighed all together. Liquids were analysed by GC/MS. All compounds present in liquids were identified by using a computerised library of mass spectra. Tri and tetramethylbenzenes were accounted for as "alkyl-benzene" and all the compounds chromatographied between naphthalene and phenanthrene were accounted for as "2-3 rings". Quantitative composition of liquids was determined by the internal standard method using octane as the internal standard.

RESULTS AND DISCUSSION

If there is no interaction between the components of the mixture, the yields obtained in the co-pyrolysis (experimental values) should be equal to the sum of yields obtained in the pyrolysis of the individual components (theoretical values). In this way, by comparing experimental and theoretical values, the existence of a synergetic effect in the yields of the most interesting pyrolysis products and the influence of the experimental conditions have been evaluated. First the evolution of the char, liquid and gases yields as a whole was studied and after that, the yields of the most interesting gaseous products and the evolution of the liquid fraction was evaluated.

Evolution of synergism with temperature

The 70/30 mixture was copyrolyzed at 600, 650 and 700ºC. At 600ºC the experimental char yield is higher than the theoretical one and there is an experimental decrease on liquid and gases production compared with the theoretical one. Analysing the evolution of the individual products only a higher experimental yield is observed for CO_2, SH_2 and methane. This fact can be related with the enhancing of cross-linking reactions that favour the evolution of this kind of gases as a by-product of char formation[11,12]. At 700ºC although there is a better liquid production than working at 600ºC and even the experimental yields of some interesting gaseous products are higher than the theoretical ones, the experimental char production is also very high.

Figure 1 show the comparison between the experimental and theoretical yields obtained working at 650ºC. It can be observed from this figure that the theoretical and experimental char yields are almost equal and that the experimental liquids yield increase in detriment of the gases one after the co-pyrolysis of the mixture. The comparison between the experimental and theoretical yields of the individual components of the gas fraction shows that there is a decrease in the experimental yield of carbon oxides and SH_2 and that on the other hand, the experimental yields for light olefins: ethylene, propylene and C_4 olefins are higher than the theoretical ones and so that, a favourable synergetic effect is observed. At 650ºC there is also an important synergetic effect for the production of all aromatic compounds, specially for benzene derivatives.

During pyrolysis of hydrocarbon nature materials[1,13] two types of reactions are suggested: first degradative processes that produce small radicals and then recombinative reactions were this small radicals take part. When secondary reactions happen via Diels-Alder, aromatic compounds are obtained. This seems to be a good explanation for 70/30 mixture behaviour: first PR is degraded and due to its high aliphatic fraction[1] it leads to a great ethylene and other light olefins production. Then the ethylene radical reacts in gas phase with the small radicals obtained from coal and so that, BTX experimental production increases. In summary it can be concluded that the main objectives of this work are achieved, working with mixtures in a mass ratio of 70/30 at 0.1MPa and 650ºC.

Evolution of synergism with pressure

All runs studying the evolution of yields with pressure were carried out at 650ºC. The good results obtained working at atmospheric pressure and 650ºC do not occur when pressure increases. There are no important differences between working at 0.5 or 1MPa. Figure 2 shows the comparison between the theoretical and the experimental yields obtained at 1MPa. The experimental char yield is higher than the theoretical one, in detriment of gases and liquids yields. The evolution of the individual components of the gas phase shows that there is no synergetic effect for any of the interesting compounds. Moreover this, working at high pressure the liquid fraction could not be evaluated. The liquids obtained have very high water content and solid suspensions and for that reason they could not be chromatographied. So, increasing pressure seems to disfavour gas phase reactions, probably because intraparticle reactions that lead to an increase on char yield[14] are enhanced.

Evolution of synergism with petroleum ratio in the mixture

Figure 3 shows the comparison between the theoretical and the experimental yields obtained for the 50/50 mixture working at 0.1MPa and 650ºC. It can be observed an important increase in the experimental char yield comparing with the theoretical values which contrast with the similar experimental and theoretical values obtained for the 70/30 mixture. There is also a slight

experimental increase for the production of CO_2, SH_2, methane and ethylene but the most important fact that should be taken into account is the bad results obtained for the liquid fraction. The only synergetic effect happens for the higher weight aromatic compounds. For benzene, toluene, xylene and alkyl-benzenes, the theoretical yields are higher than the experimental ones. From these results it can be concluded that the increase in the petroleum residue ratio in the mixture disfavours tar forming reactions while enhances char formation. One of the suggested explanations for the behaviour of the 50/50 mixture is that although PR degradation occurs, when PR mass ratio in the mixture increases, the formed radicals can not react with the radicals emerging from coal and this way secondary reactions in gas phase that lead to the BTX formation are not allowed, and only intraparticle reactions that increase char formation are enhanced. A more detailed study of these processes and probably the analysis of the nature of chars obtained would provide enough information to consolidate the present explanation.

REFERENCES

1. Ofosu-Asante K., Stock L.M, Zabransky R.F. (1989). Fuel. Vol.68, 567-572.
2. Hayashi J., Kawakami T., Taniguchi T., Kusakabe K., Morooka S. (1993). Energy&Fuels, 7, 1118-1122.
3. Miura K., Mae K., Asaoka S., Hashimoto K.(1991). Energy&Fuels, 5, 340-346.
4. Fontana A., Braekman-Danheux C., Laurent P. (1995). "Coal Science and Technology 24".(Elsevier. J.A. Pajares, J.M.D. Tascón Eds.) pp 1089-1092.
5. Laurent P., Braekman-Danheux C., Fontana A., Lecharlier M. (1997). ICCS 97. Vol II. (Ziegler et al Eds.), 837-840.
6. Palmer S.R., Hippo E.J., Tandon D., Blankenship M. (1995). "Coal Science and Technology 24".(Elsevier. J.A. Pajares, J.M.D. Tascón Eds.) 29-33.
7. Klose W., Stuke V. (1993). Fuel Processing Technology, 36, 283-289.
8. Moliner R., Suelves I., Lázaro M.J. (1998). Energy&Fuels. Vol.12, N°5, 963-968.
9. Suelves I., Lázaro M.J., Moliner R.(1997) ICCS 97. Vol. II 745-748 (Ziegler et al Eds.)
10. Moliner R., Lázaro M., Suelves I. (1997). Energy&Fuels. Vol.11, N°6, 1165-1170.
11. Ibarra J.V., Cervero I.,García M., Moliner R.(1990). Fuel Processing Technology, 24, 19-25.
12. Suuberg E.M., Lee D., Larsen J.W.(1985). Fuel. Vol.64, 1668-1671.
13. Moliner R. (1995). Final Report Project CECA 7220-EC/763.
14. Moliner R., Ibarra J.V., Lázaro M.J. (1994). Fuel. Vol.73, n°7, 1214-1220.

Figure 1. Experimental and theoretical yields: Samca/RP (70/30). P=0.1MPa. T=650ºC.
A) Mass balance

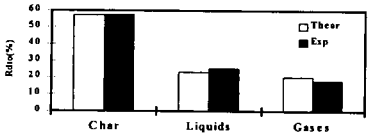

B) Gases

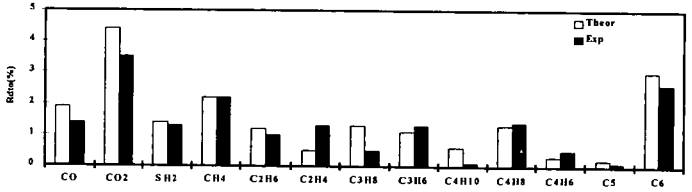

C) Liquids

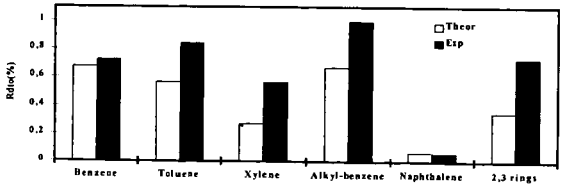

Figure 2. Experimental and theoretical yields: Samca/RP (70/30). P=1MPa. T=650°C.
A) Mass balance

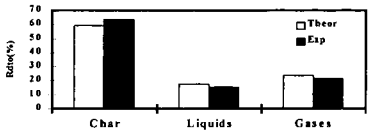

B) Gases

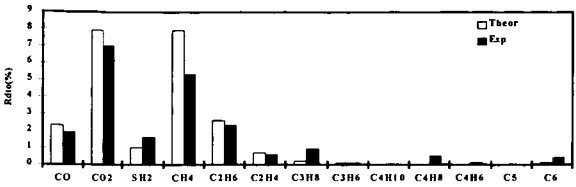

Figure 3. Experimental and theoretical yields: Samca/RP (50/50). P=0.1MPa. T=650°C.
A) Mass balance

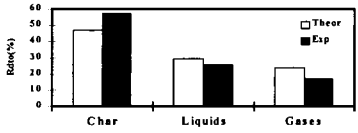

B) Gases

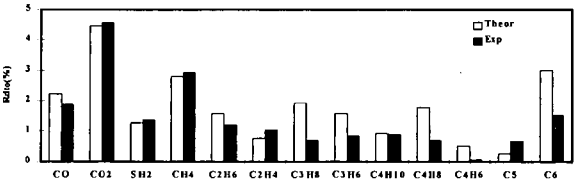

C) Liquids

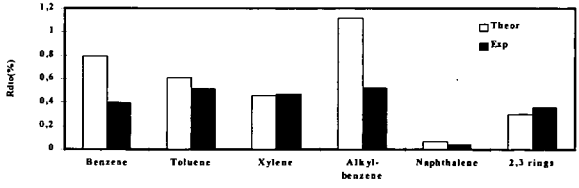

THERMAL CRACKING PROPERTY OF MARLIM VACUUM RESIDUE

Teruo Kondo[1], Shinya Sato[1], Akimitsu Matsumura[1], Ikuo Saito[1]
Albertino Machdo de Carvlho[2], Wladimr Ferraz de Souza[2]

[1]National Institute for Resources and Environment
16-3 Onogawa, Tsukuba, Ibaraki, 305-8569 Japan

[2]PETROBRAS Research and Development Center
Cidade Universitaria Quadra 7 s/n CEP 21949-900
Rio de Janeiro, Brazil

Keywords : Marlim residue, Thermal cracking, coking, asphaltene structure

INTRODUCTION

The world-wide demand for transportation fuels and light fraction oils is expected to increase steadily, while the world supply crude has become rather heavier. Therefore, development of the upgrading technology of heavy oils is very important. However, upgrading of heavy oils is generally very difficult because of serious problems such as coke formation and catalyst deactivation. These problems are mainly caused by asphaltene in heavier oil. In catalytic hydrocracking of heavy oils, asphaltenes are known to be the most refractory. It is profitable for the progress of upgrading of heavy oils such as vacuum residue to understand the reaction behavior of asphaltene cracking. Many investigators provide ample information about pathways, kinetics and coke formation mechanism in the thermal cracking of asphaltenes or residues[1-9]. The purpose of this study is to clarify thermal cracking behavior of Brazilian Marlim vacuum residue, its asphaltene and deasphalted oil. Marlim crude is Brazil off-shore of large scale reservoir and a typical heavy oil. The vacuum residue in Marlim crude is as many as 30-33% and has high asphaltene contents.

EXPERIMENTAL

Feed materials used in this study were Marlim vacuum residue(MLVR) and the asphaltene (MLVR-AS) and the deasphalted oil (MLVR-DAO) obtained from MLVR. MLVR-AS was precipitated with excess of n-heptane (40:1), stirred for 24 hours and separated with a centrifuge. Finally, the asphaltene was dried under vacuum at 50°C, for 24 hours. MLVR-DAO was obtained from n-heptane solubles by removing n-heptane with evaporator.

A 110 ml batch autoclave with magnetic stirrer was used in the thermal cracking. An autoclave was loaded with 3 g of feed and 15 g of decalin as solvent and pressurized to 1 MPa of nitrogen gas and heated up to the reaction temperature(400-440°C) at 10°C/min. After holding at reaction temperature for the desired time(0-90 min), the autoclave was cooled down to room temperature and gases were vented off and analyzed by gas chromatography. The reaction products in the autoclave were separated into the oil and the solid products by suction filtration.The solid product was extracted with toluene using ultra sonic. Toluene insoluble material in the solid product was defined as coke.

^{1}H and ^{13}C NMR were measured using JEOL Lamda 500. The conceptual structure model of asphaltene samples were deduced from the structural parameters obtained from NMR, elemental analyses and average molecular weight with the proposed by Sato's method[10].

RESULTS AND DISCUSSION

The properties of three Marlim samples (MLVR, MLVR-DAO and MLVR-AS) and Arabian Light vacuum residue asphaltene (ALVR-AS) are shown in Table 1. Nitrogen content of MLVR-AS is about twice of DAO and nitrogen is concentrated in the asphaltene fraction. On the other hand, sulfur contents of asphaltene and deasphalted oil are almost the same. On the comparison between MLVR-AS and ALVR-AS, nitrogen content of MLVR-AS is higher than ALVR-AS, but the content of sulfur and vanadium is lower than ALVR-AS. H/C atomic ratios and fa of MLVR-AS is similar to ALVR-AS.

Coking property of MLVR, MLVR-DAO and MLVR-AS are shown in Figure 1. Coke yield from MLVR-AS increased rapidly from 410°C of cracking temperature. In contrast, the coke formation from DAO did not take place even 420°C. But asphaltene were observed to form in the product oil after thermal cracking of MLVR-DAO. The coke yield from MLVR corresponded to the total amount of coke generated from asphaltene fraction and maltene fraction in MLVR. Asphaltene fraction are easily caused the coke formation during the thermal cracking.

Figure 2 shows the relationship between the reaction time and the coke yield in thermal cracking of MLVR-AS at the various temperatures. When cracking temperature was 410°C, The coke formation was not observed until 30 min of the reaction time and seemed to have an induction period. On the other hand, at higher temperature (430, 440°C), coke was formed rapidly at high rate without an induction period. This tendency was observed in thermal cracking of ALVR-AS[11].

Gas yield from MLVR-AS cracking is shown in Table 2. H_2 and hydrocarbon gases increased with an increase of reaction severity (temperature and time). It seems that coking of asphaltene progresses attended with dehydrogenation and dealkylation. A small amount of CO and CO_2 were observed in the generated gases. CO_2 yield was almost constant regardless of the reaction conditions. CO_2 formation suggests asphaltene molecule has carboxylic functionality and decarboxylation is finished at the initial stage of the reaction.

The composition and structure of original asphaltene were changed with thermal cracking. Elemental analyses and molecular weight and NMR spectra of reacted asphaltene were measured. The H/C atomic ratios and molecular weight of reacted asphaltenes decreased with an increase of the cracking temperature (Figure 3). Especially, the molecular weight of reacted asphaltene decreased rapidly with an increase of the reaction severity. Structural parameters of original asphaltene (MLVR-AS) and reacted asphaltene are shown in Table 3.

Figure 4 shows the conceptual model structure of original asphaltene and reacted asphaltene at 400, 430 and 440°C of the cracking temperature. As shown in this picture (figure 4), at low cracking temperature(400°C), asphaltene decomposition occurs through the cleavage of bridge chain which connects the cluster unit structure in asphaltene molecule. At higher temperature, in addition to the cleavage of bridge chain, dealkylation of alkyl substitutes connected to fused ring and dehydrogenation of naphthenic ring are found to be occurred. The reacted asphaltene obtained at 440°C was almost composed of fused aromatic ring.

CONCLUSION

This work was carried out to investigate the thermal cracking behavior of Barazilan Marlim vacuum residue.

1. Marlim vacuum residue has relatively high CCR , asphaltenes and nitrogen. Nitrogen compounds are concentrated in the asphaltene fraction. The asphaltene from VR has high aromaticity.
2. Coking reaction of the asphaltene was caused rapidly from 410°C. For deasphalted oil from VR, the formation of coke was not observed even at the temperature of 420°C.
3. Molecular weight and H/C atomic ratios of reacted asphaltene decreased with an increase of the cracking temperature. Asphaltene reacted at higher temperature shows highly aromatic structure with a little alkyl substitutes.

ACKNOWLEDGMENT

This work was supported by ITIT program of Agency of Industrial and Science Technology, MITI , Japan.

REFERENCES

1) Savage P.E., Klein M. T., Kukas S. G., Energy & Fuels, **2,** 619(1988)
2) Moschopedis S. E., Parkash S., Speight J. G., Fuel, **57** , 431(1978)
3) Truth D. M., Yasar M., Neurock M., Nigam A., Klein M. T., Kukes S. G., Fuel Sci. Tech. Int., **10,** (7), 1161(1992)
4) Del Bianco A., Panariti N., Anelli M., Beltrame P. L., Carniti P., Fuel, 72, 75 (1993)
5) Yasar M., Truth D. M., Klein M. T., Prepr. ACS., Div. Fuel Chem., **37**, (4),1878 (1992)
6) Wiehe I. A., Ind. Eng. Chem. Res., **32**, 2447(1993)
7) Kawai H., Kumata F., Prepr. ACS., Div. Pet. Chem., **42**, (2), 406(1997)
8) Shengha L., Chenguang L., Guohe Q., Wnejie L., Yajie Z., Prepr. ACS., Div. Pet. Chem., **42,** (2), 411(1997)
9) Karacan O., Kok M. V., Energy & Fuels, **11**, 385(1997)
10) Sato S ., Sekiyu Gakkaishi, **40,** (1), 46(1996)
11) Kondo T., Sato S., Matsumura A., Saito I., Proceedings of JECAT' 97, 335(1997)

Table 1 Properties of Marlim Vacuum Residues

	MLVR	MLVR-DAO	MLVR-AS	ALVR-AS*
C (wt%)	86.66	86.59	87.12	83.94
H(wt%)	10.17	10.88	8.62	7.86
N(wt%)	0.98	0.72	1.49	0.95
S(wt%)	0.90	0.88	1.04	6.72
H/C (atm)	1.40	1.50	1.18	1.12
V(ppm)	82	43	230	466
Ni(ppm)	59	33	160	128
n-C7 IS(wt%)	21.4			
C.C.R.(wt%)	22.8	15.7		
fa	0.30	0.26	0.45	0.42

* ALVR-AS : Arabian Light Asphaltene

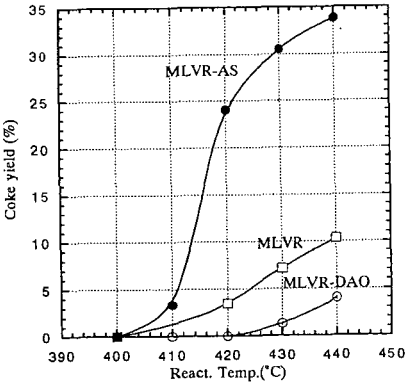

Figure 1. Coking property of Marlim vacuum residues

N2 :1MPa, Feed/DH=3/15wt, React. time : 60 min

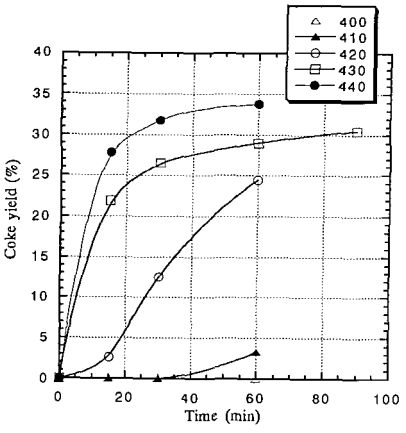

Fugure 2. Effect of reaction time on coke formation of MLVR-AS thermal cracking

Table 2 Reaction conditions and gas distribution from MLVR-AS thermal cracking

Conditions		Yield (wt%/AS)		Gas mmol/g AS × 100						
Temp.(°C)	Time(min)	Coke	Gases	H_2	CH_4	C_2H_6	C_3H_8	$C_2H_4+C_3H_6$	CO	CO_2
440	15	27.8	2.6	44	62	15.0	7.7	7.0	4.0	1.8
	30	31.8	3.3	63	83	19.7	10.0	8.0	4.0	1.8
	60	33.8	4.4	113	123	28.3	13.7	9.4	4.3	2.0
430	15	21.9	2.0	27	50	10.7	5.3	5.0	3.3	2.0
	30	26.5	2.4	42	62	14.3	6.7	4.0	4.0	2.0
	60	29.7	3.3	71	86	20.2	9.7	8.0	4.3	2.0
420	15	2.6	1.1	20	28	6.0	2.7	1.3	3.0	1.8
	30	12.7	1.4	31	36	7.7	3.3	2.0	3.3	1.7
	60	24.4	2.1	86	56	12.0	5.7	2.7	3.3	1.9
410	15	0.0	0.7	14	19	4.0	1.7	1.4	2.3	1.8
	30	0.0	0.8	12	18	3.7	1.7	1.4	2.7	1.8
	60	3.3	1.1	27	30	6.0	2.3	1.3	3.0	1.8
400	15	0.0	0.3	3	7	1.3	0.6	0.0	1.7	1.6
	30	0.0	0.5	9	11	2.3	1.0	0.8	1.6	1.6
	60	0.0	0.7	14	18	3.7	1.3	1.0	2.0	1.8

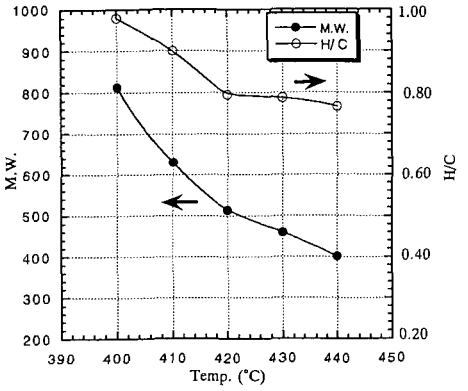

Figure 3. Effect of cracking temperature on molecular weight and H/C of reacted asphaltene

N2 : 1Mpa, MLVR-AS/DH=3/15wt, React. time 60 min

Table 3 Structural Parameters of MLVR-AS and reacted asphaltene

Parameter	MLVR-AS	Cracking temp. (°C)		
		400	430	440
H/C	1.19	1.03	0.79	0.76
M.W	1730	813	459	401
fa	0.45	0.55	0.66	0.88
Ct	128	61	35	31
Ht	152	63	28	24
Car	58	34	24	24
Har	16	10	9	9
H_α	26	15	6	6
H_β	83	28	10	6
H_γ	27	11	3	3
M	3.0	1.5	1.0	1.0
Rt	24.0	13.0	10.0	8.0
Ra	15.0	9.0	6.0	7.0
Rn	9.0	4.0	4.0	1.0
Cap	34.0	19.0	14.0	12.0
Ctr	81.0	43.0	33.0	27.0
N	9.2	4.5	1.0	2.0
l	5.2	3.9	2.0	2.0

Ct : Number of total carbon
Ht : Number of total hydrogen
Car : Number of aromatic carbon
Har : Number of aromatic hydrogen
H α : Number of hydrogen α to aromatic rings
H β : Number of hydrogen β to aromatic rings
H γ : Number of hydrogen γ to aromatic rings
M : Number of fused ring units
Rt : Number of total rings
Ra : Number of aromatic rings
Rn : Number of naphthenic rings
Cap : Number of peripheral carbon of aromatic rings
Ctr : Number of total carbon of fused rings
N : Number of paraffinic chain
l : Average chain length

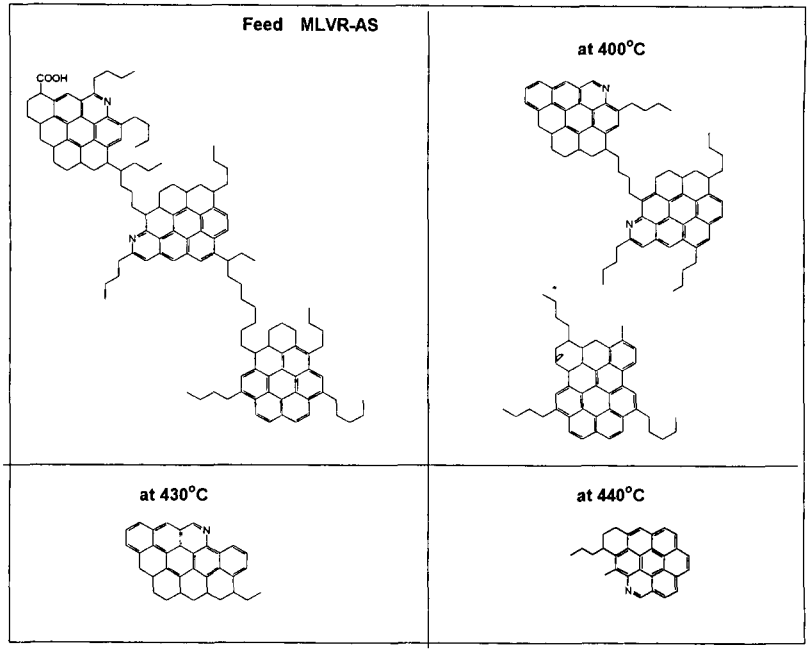

Figure 4. Strucutural Change of MLVR-AS in Thermal Cracking

INDUSTRIAL GAS TURBINE FUEL SURVEY-BASIC PROPERTIES

Bruce Rising
Siemens Westinghouse Power Corporation
4400 Alafaya Trail
Orlando, Florida 32826-2399

Keywords: Fuel, Gas Turbine, Emissions

ABSTRACT

In the last few decades, the quality of industrial feedstocks to refineries has continued to decline. Here in the United States many of the large remaining petroleum reserves are high in aromatics and sulfur content, while at the same time environmental standards call for lower sulfur in all fuel classes, and reduced aromatics in the large volumes of gasoline produced. These competing requirements force refineries to upgrade the feedstocks more aggressively in order to comply with the stricter environmental standards. This is particularly true of feedstocks coming from the west coast, or the Alaskan North Slopes. The impact of these lower quality feedstocks is expected to impact the quality of the final products available.

To ascertain the general quality of industrial fuels used in gas turbines, a survey of liquid fuels was undertaken. The purpose of the fuel survey was to characterize the properties of both domestic and international fuel supplies using a battery of test methods. This information would be used in estimating the fuel performance in an industrial gas turbine. Fuel properties of key interest were sulfur content, boiling point distribution, chemical constituents, ash content, and smoke point.

The survey required fuel samples from both domestic and international sources. Samples of fuel were taken from multi-product pipelines, bulk terminals, on-site storage facilities, and vendor supplied stocks. The bulk of the testing techniques employed were based on standardized ASTM methodologies. The scope of testing was greatly expanded beyond the normal fuel qualifications employed for industrial fuel characterization.

Results showed confirmation of the US EPA's regulatory efforts to reduce fuel sulfur levels to less than 0.05 wt%. However, there was not a significant difference between the sulfur levels of the higher grades of No. 1 type fuels (kerosine blends) and that of the more widely available No. 2 grade distillates.

The No. 2 grade distillates available in the US also showed a higher aromatics content than equivalent grades selected from international sources. This appears to be due to refinery processes in the US that are designed to optimize the gasoline yield from the refinery, resulting in higher aromatics content in some distillate streams.

INTRODUCTION

An industrial fuel survey was undertaken to understand potential changes in the quality of fuels available in the commercial markets. Of specific interest were fuel properties that might result in less than ideal performance when used in industrial gas turbine applications.

Historically, gas turbines have been well known for the ability to effectively use fuels of wide ranging characteristics and properties. Where reciprocating engines are impacted by the ignition quality of the fuel, or require a specific vapor pressure to burn, gas turbines do not typically exhibit sensitivity to fuel ignition properties. From an operating point of view, as long as the fuel can reach the fuel nozzle, and atomize properly, the only significant characteristic of concern is the presence of metals. Metals in the fuel, particularly alkaline and alkaline-earth elements are especially aggressive in their attack of hot metal surfaces. Therefore the metals content is often very tightly specified and controlled.

Advance turbines designed for low NO_x emissions have unique fuel hardware designs. Conventional designs consist of a pressure atomizing orifice type nozzle. The design is very forgiving, as well as easily manufactured and easy to repair. However, stricter environmental requirements have forced fuel system designers to develop improved atomization and mixing to reduce emissions, with an emphasis on NO_x. In some cases, the newer designs may impose more stringent requirements on the fuel. Determining a relationship between fuel properties and a system design was one of the long term goals.

METHODS

Standard ASTM[1] test methods were used extensively to evaluate fuel properties for this test program. No new methods were developed specifically to support these efforts. Other techniques which were also used include GC analysis of the fuel hydrocarbon structures.

Fuel samples were collected from various sources, placed in teflon bottles, and then shipped by overnight courier to the laboratories for analysis. Sample chemical analysis was usually completed within seven days after collection.

RESULTS

The test results are summarized by fuel grade (or type). In general, there were three grades of fuels identified:

1) No. 1/Jet A/Kerosene, but not including JP-5 grades
2) No. 2 distillate (including No. 2 fuel oil and diesel oils)
3) Gas-oils. Fuels similar to No. 2 based on ASTM classification, but with a wider distillation range, typically an endpoint that is greater than 700°F.

In addition, a reference highway No. 2 diesel fuel was used as a benchmark. This fuel sample was found to maintain relatively consistent analytical chemical properties from source-to-source, and from year-to-year.

The first comparison made is to summarize all of the fuels on a single chart, showing their boiling point range as a function of the percentage of the fuel distilled. From this chart, it is possible to clearly distinguish the specific grades of fuels just described. At the bottom of the chart lies a cluster for the No. 1 grade fuels. These are the kero-jet grades, widely available within the United States, but not the first fuel of choice for industrial applications because of the higher costs often associated with this transportation grade fuel.

The next cluster on the chart shows the No. 2 grade fuels. These fuels comply with the ASTM requirement that 90% of the fuel must be distilled at temperatures less than 640°F. In close proximity to the No. 2 grade fuels are the gas-oils, with a unique boiling point distribution. The gas-oils are identified primarily by the higher final boiling point which is exhibited on the right hand side of the figure.

Fuel Sulfur Analysis

Here in the United States, fuel is often hydro-treated to reduce the fuel sulfur levels. EPA requirements in the US have established diesel fuel sulfur maximums of 0.05 wt% (500 ppmw)[2], with gasoline sulfur requirements even lower. With declining feedstock quality, it is a requirement to upgrade the fuel using hydro-treatment, a process which lowers the product sulfur content. Table 1 summarizes the average sulfur levels encountered from fuel samples taken from both domestic and international sources.

Boiling Point

The data in Figure 1 show the clear delineation between the three types of fuels tested in this program. (Table 2 summarizes the endpoint analysis extracted from that data.) This figure shows that the end points on the gas-oils, samples collected from overseas sources, are distinctly different from comparable No. 2 grade fuels available in the United States.

Based on field test data, the effect of the higher end points for the gas-oil type fuels is expected to result in a higher smoke/particulate emissions than a lower boiling point fuel. A rule-of-thumb has been to require fuels with an end point that is less than 700°F in order to minimize the formation of a visible smoke plume, particularly at reduced loads.

Hydrocarbon Types

Hydrocarbon types were evaluated by two different methods: ASTM D 5291 and by chromatography. The general hydrocarbon classifications of interest are aromatics, olefins, and saturates determined using ASTM D 5291. The results of the analysis are summarized Table 3.

These are the results of 15 samples tested. The bulk of the US fuel samples exhibit saturates which are less than the average value shown in (70% for the average US values). All of the international fuel samples, with one exception, have higher saturate levels than the average shown in Table 3. A similar statement could be made for the aromatics, except that in this case, the lower aromatics tend to be clustered with the international fuel types (and the Jet A kerosines), while the higher aromatics are centered among the domestic grades of fuel (28.5%).

This appears to be consistent with the processing technologies associated with US refineries, and the limitations on aromatic hydrocarbons in the gasoline pool. Here in the US feedstocks are extensively upgraded to increase gasoline yields. This results in blending with Light Cycle Oil at the refinery that can produce very high concentrations of aromatics in the distillate streams. In addition, there are limits on the maximum aromatics content in the gasoline streams This requires that the excess aromatic components be re-distributed, and the distillate stocks targeted for stationary applications is the most convenient outlet.

For highway diesel and aviation kerosine applications aromatics more tightly controlled maintain cetane levels (for diesel fuels) and to meet aromatic specifications (for aviation applications). However, in the distillate heating oil market, there is no specific aromatic or cetane requirement for these fuels. Thus there would be a tendency to let the higher aromatic contents collect in this refinery stream.

In overseas markets there is still continued use of straight run distillates in large quantities. Also, Cetane improvers are not as widely used outside the United States. So the refinery stream for the distillates reflects a higher saturates and lower aromatics content than in the US.

Chromatography was used to further distinguish the chemical constituents that make up the fuel products. These are summarized in Figure 2. These results also show that the international grades clearly show lower aromatics, and higher paraffinic content that domestic US blends. Also, a high grade No. 2 highway diesel fuel is shown on the chart.

Ash Content

As expected, all samples tested showed ash contents that were reported at levels at or near the detection limits. The detection limits for ash using ASTM D 482 is reported to be 0.001 wt%; however, lower levels of detection are possible by using larger fuel sample volumes. In this program this was done to achieve the minimum detection levels reasonably achievable. The industry average of all fuel samples is 0.0015 wt% (15 ppmw). The significance of accurate ash measurement will be discussed in the next section.

Property Comparison: No. 1 and No. 2 Grades

Other relevant fuel properties were determined in addition to those described in previous section. A summary of those results is provided in Table 4.

DISCUSSION

The results show that US blends of both No. 1 and No. 2 fuels with sulfur levels consistent with the mandated US EPA requirements of 0.05 wt% maximum. While the average value shown in the table is slightly higher than that required by the EPA, the mean value is substantially influenced by a single sample which has a fuel sulfur level of 0.155 wt%. Removing this sample from the database lowers the average value to less than 0.043 wt%, meeting the US EPA requirements for fuel sulfur.

No. 1 Fuel

Results of the No. 1 fuel survey show excellent low sulfur characteristics. However, these fuels are substantially Jet A grade fuels (API gravity greater than 37 and 90% point is less than 540°F). Interestingly the No. 1 fuels show a broader boiling point range (exhibit a higher standard deviation) than the domestic No. 2 fuels. This is of virtually no impact with regard to fuel performance, although initial expectations were that the No. 2 fuel would likely exhibit the greater dispersion of the two fuel types.

International Fuel Grades

There is a clear trend toward the use of wider boiling point fuels in markets outside the United States and Canada. This was first observed by the author from fuel survey's conducted in Europe in the early 1990's. Higher end points were frequently found for distillate oils sold into the industrial/consumer markets. These fuels often did not meet the specific requirements established by the ASTM for No. 2 grade fuel (ASTM D396, D2880 or D375). The general performance of these fuels is expected to be similar to those of No. 2 grade fuels. However, there are some distinct differences to be expected. One of the most evident would be the production of a visible smoke plume. This phenomena has been associated with the liquid fuels exhibiting an endpoint that is 700°F or higher. This endpoint is reached or exceeded for most fuels similar to No. 2 distillate that are available in the international markets (Europe, Asia, South America).

In Germany, two grades of this fuel are available for general consumption. They are classified as IGO (Industrial Gas Oil) and AGO (Automotive Gas Oil). The AGO cut exhibits a lower endpoint, and less smoking tendency, than the IGO product. The features associated with AGO (reduced final boiling point) produce a less visible exhaust plume when burned in power applications.

ENVIRONMENTAL IMPACT

Certain fuel properties clearly affect their environmental performance. Fuel bound sulfur and nitrogen are the two of the most important. However, test results in this program have shown that both the domestic and international fuels exhibit very low sulfur levels, and would produce SO_2 emissions that would be difficult to measure during exhaust emission testing.

Not so clear is the impact of other fuel qualities, such as aromatics content, smoke point, and ash. These specific fuel properties, as well as others, can impact the formation of smoke, particulates, and a visible plume. Distinguishing particulates between carbon/organic and inorganic (or ash) components is difficult to predict. However the inorganic ash component is the easiest of the two to estimate. The laboratory results from ASTM D 482 are assumed to represent the same ash constituents that would be released into the environment. For a large industrial gas turbine, using 100,000 lb/hr of liquid fuel consumption, a test analysis with detection limits of 0.01 wt% would produce an expected particulate emission rate of 10 lb/hr (0.0077 lb/MMBtu, HHV basis), based solely on the ash constituents. There is no straightforward mechanism for estimating the additional particulates due to the carbon/organic fraction. But evidence from field tests clear shows that fuels with final boiling points in excess of 700°F can, under the proper set of conditions, produce a visible plume.

Based on the test results from this program, using the same conditions just described would result in particulate emissions due to the ash content of the fuel at approximately 1.5 lb/hr (0.00077 lb/MMBtu, HHV basis). This level of particulates would produce no visible plume, and would be extremely difficult to measure using standardized test methods.

CONCLUSION

Fuel sulfur levels within the United States reflect the impact of federal legislation mandating sulfur reductions to less than 0.05 wt% (500 ppmw). Only in one instance was a fuel for gas turbine applications identified with a sulfur content greater than this.

US fuels are substantially dominated by higher aromatics and lower saturate contents than comparable non-domestic grades of fuels (excluding the Jet A kerosine grades). The higher aromatic contents may result in greater particulate emission, or possibly a visible smoke plume. International samples show trends of higher saturates and lower aromatics, somewhat similar to the general hydrocarbon information identified for Jet A grades of fuel.

Ash contents of all fuel samples tested were very close to the detection limits of the test method. An average value of 15 ppmw was reported.

These results, as well as additional test parameters being considered, will eventually be used to develop more useful and effective fuel specifications for industrial gas turbine applications.

ACKNOWLEDGMENTS

This work could not have been completed without the help of Phil and Nader Sorurbakhsh of Texas Oil Tech Laboratories, in Houston, Texas.

REFERENCES

[1] ASTM 100 Barr Harbor Drive, West Conshohocken, Pa. 19428

[2] US EPA 40 CFR 80.29. Beginning 1 Oct 93 sulfur is limited to 0.05 wt% for highway diesel.

[3] "A Comparison of Low and High Sulfur Middle Distillate Fuels in the United States", J. Andrew Waynick, 215th ACS National Meeting, Dallas, TX. March 29, 1998

Table 1 Measured Fuel Sulfur Levels (ASTM D4294)

Fuel Type	Average	Minimum	Maximum	Standard Deviation
No. 1	0.0207	0.003	0.0322	0.0119
No. 2	0.0535	0.025	0.155	0.035
Amoco Fuel Analysis (1994)[3]				
Low Sulfur Diesel	0.0296			0.0092
High Sulfur Diesel	0.2082			0.0902

Table 2 Boiling point distribution

	End Point		50% Point		90% Point	
	Average, °F	SD	Average, °F	SD	Average, °F	SD
No. 1	540.8	17.1	424.7	12.8	493.4	15.8
No. 2	657.1	7.8	511.4	11.7	607.6	7.3
Gas Oil	693.6	23.5	538.9	8.7	647.9	21.4

Table 3. Fuel classification by hydrocarbon types (ASTM D 5291)

	Hydrocarbon Analysis by Volume % (All Fuels Tested)			
	Olefins	Aromatics	Saturates	Smoke Point
Average	1.13	23.06	75.80	18
Standard Deviation	0.472	6.982	7.127	3.0
Maximum	2.3	35.8	84.92	23
Minimum	0.39	14.2	62.4	12

Table 4 General fuel properties

	No. 1/Kerosene	No. 2 Distillates
Flash Point, °F	144	160
Pour Point, °F	-59	-8
Kinematic Viscosity @ 104°F (cSt)	2.08	3.03
Specific Gravity	0.82	0.854
LHV, Btu/lb	18,526	18,327
HHV, Btu/lb	19,747	19,446
Carbon Content, wt%	86.22	86.71
Hydrogen Content, wt%	13.57	13.05
Oxygen Content, wt%	0.16	0.13
Nitrogen Content, wt%	0.0078	0.018
Sulfur Content, wt%	0.0322	0.0535

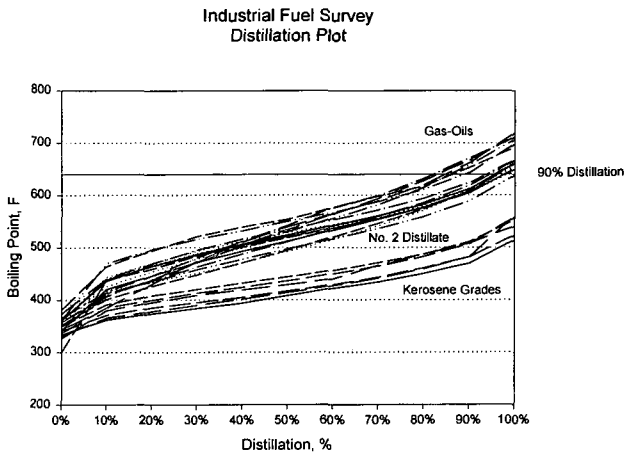

Figure 1. - Boiling Point Distribution for Three Fuel Grades

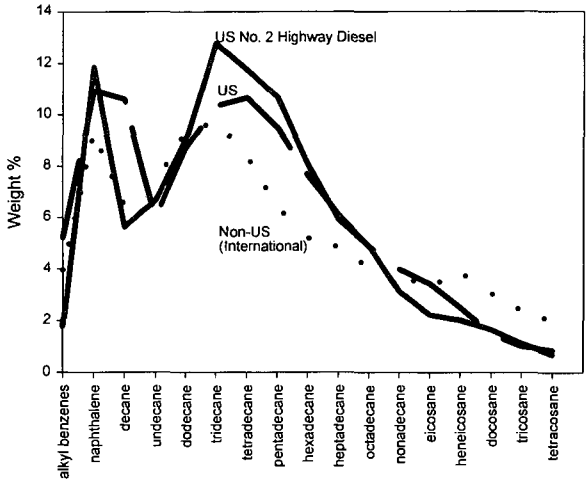

Figure 2. - Fuel Chromatography Analysis.

SUPPRESSION OF PYROLYTIC DEGRADATION OF N-ALKANES IN JET FUELS BY HYDROGEN-DONORS

John M. Andrésen, James J. Strohm, Michael M. Coleman and Chunshan Song*
Applied Catalysis in Energy Laboratory, The Energy Institute
The Pennsylvania State University, University Park, PA 16802.

KEYWORDS: Pyrolysis, thermal stability, aviation jet fuels.

ABSTRACT

The pyrolytic degradation of alkanes in jet fuels can be extensively reduced by adding suitable hydrogen donors, that suppress the formation of free radicals. Accordingly, this paper characterizes the chemical interactions between n-tetradecane and the hydrogen donors benzyl alcohol and 1,2,3,4-tetrahydro-1-naphthol. The hydrogen donors produced the expected overall enhancement on the liquid yields and reduced cracking of the n-tetradecane. The observed suppression of pyrolytic degradation was strongly related to a reduction in the alkane products adding benzyl alcohol, but the 1,2,3,4-tetrahydro-1-naphthol indicated an initial decrease in the alkenes.

INTRODUCTION

The use of hydrogen donors to suppress pyrolytic degradation of jet fuels (1-3), is a potential route to reach the JP-900 thermal stability requirement set up by the US Air Force (4). Since the fuel also functions as the main coolant for the different electronic and system components of the aircraft, the fuel temperatures may increase up to 480°C (900°F) and thermal stability to obtain reduced solid deposition is a key element in this research (5). The pyrolytic conversion of alkanes, typically found in petroleum derived jet fuels, is generally considered to involve the formation of free radicals (6). The propagation of these reactive intermediates results in a broad distribution of smaller alkane and alkene units, and triggers the aromatization of the liquid, which leads to undesirable solid depositions. As a solution, the free radicals can be halted right after the initiation step by the use of hydrogen donors (1-3). However, the chemistry involved in inhibiting free radical reactants during thermal degradation of fuels is not fully understood. This is addressed in this study, where the suppression of reactive intermediates between the n-alkane, n-tetradecane, and the hydrogen donors benzyl alcohol and 1,2,3,4-tetrahydro-1-naphthol, has been characterized.

EXPERIMENTAL

The compounds used were n-tetradecane (TD, Aldrich 99%), benzyl alcohol (BA, Aldrich 99.8%) and 1,2,3,4-tetrahydro-1-naphthol (THNol, Acros 97%). Stressing of TD alone or in different mixtures with BA or THNol were performed for 30 minutes in a fludized sandbath at 425, 450 and 475°C. A detailed description of the experimental setup and analytical determination of the product distribution using GC and GC/MS, has been reported elsewhere (1, 5).

RESULTS AND DISCUSSION

The liquid yields for the n-tetradecane (TD) stressed alone at 425, 450 and 475°C and its mixture with 0.5, 1, 3 and 5 mole% benzyl alcohol (BA) and 1,2,3,4-tetrahydro-1-naphthol, are plotted in Figure 1. The amount of gaseous products is scarce at 425°C, yielding only around 2 wt%. However, adding 0.5 mole% of either BA or THNol resulted in a marked increase in the liquids (Figure 1). At 450°C, the liquid yields are still high and the same initial rise in remaining liquid is observed with the addition of only 0.5 to 1 mole% of hydrogen donors. Rising the temperature to 475°C resulted in a significant decrease in the liquid yields. Still, the more dramatic enhancement in the liquid yields was observed after the

addition of 1 mole% of the hydrogen donors. When comparing the increase in liquid yields at the three temperatures for TD alone and with 1 mole% addition of BA or THNol, there is a significantly rise from around 1-2% at 425°C to 4-6% at 475°C, as an effect of hydrogen donors. Scheme 1 presents in a simplified manner the role of the hydrogen donors in the thermal stabilization of the fuel. The n-tetradecane is cracked due to the influence of heat into two primary radicals. The additive can cap a radical at this stage, preventing the propagation of the reaction and leaving a n-alkane product. However, if the radical is not stopped, it will abstract a hydrogen from another TD molecule. This may leave a primary radical on the TD, which yield a n-tetradecane upon stabilization. More likely, a secondary radical will be formed. Through β-scission, the secondary radical will yield a 1-alkene and a primary radical product. The extent of this cyclic process can be monitored through the concentration of 1-alkenes (in bold). The primary radical capture has been reported in the literature to be the main target for benzyl alcohol (3). However, the ability of hydrogen donors to aim specially at secondary radicals has not been described.

The ability of the hydrogen donor to capture any of the radicals will hinder the propagation reaction, resulting in an increased ratio of remaining TD in the liquid product, when compared to that initially used. Figure 2 compares this relationship for n-tetradecane at the three temperatures 425, 450 and 475°C with the addition of 0.5 to 5 mole% of THNol. Clearly, as the temperature is increased, the TD remaining over that initially is decreasing for the TD stressed alone, from about 85 mole% at 425°C to around 30 mole% at 475°C. At the three different temperatures, there is a sharp initial rise in the TD remaining content with the addition of only 0.5 to 1 mole% of THNol, similar to that found for the liquid yields. However, as the temperature becomes more elevated, a further slow increase is also observed for the addition of THNol up to 5 mole%. For BA, a similar temperature and concentration dependence was found, in accordance with that previous reported for BA at 450°C (3).

The n-alkane and 1-alkene product distributions for the series of THNol addition at 450°C are shown in Figures 3 and 4, respectively. With the addition of 0.5 mole% THNol, there is a decrease in both the alkane and alkene gaseous products (C1 to C3) in accordance with the observed increase in liquid yield (Figure 1). However, for C4 and higher there is a marked decrease in the 1-alkene products (Figure 4), when adding only 0.5 mole% THNol. The n-alkanes from C4 and higher for the TD alone and with 0.5 mole% THNol show a similar product distribution. Referring back to Scheme 1, the THNol seems to target the secondary radicals at this low concentration. Increasing the THNol concentration appears to enhance the ability of the THNol to target primary radicals as well, resulting in a steady decrease of n-alkane products (Figure 3), as the 1-alkene concentration is decreasing at a lower rate. The selective targeting of secondary radicals has also been indicated from the GC analysis of the liquid products from TD/THNol mixtures at 475°C. Figure 5 shows the ratio of the 1-alkene peak area over that of the corresponding n-alkane for TD alone and with 0.5 mole% THNol and BA addition. There is a clear reduction in the alkene/alkane ratio for the THNol mixture, supporting the finding that THNol is targeting secondary radicals at low concentrations. In addition, Figure 5 shows that BA is mainly targeting the primary radicals at 475°C, as illustrated by the relative decrease in the n-alkane peaks in comparison to that of the 1-alkenes. The different reaction mechanisms for the different hydrogen donors may result in synergistic effects from mixing small amount of both stabilizers, where each has the task of capping different radicals.

CONCLUSIONS

The most significant effect of benzyl alcohol (BA) and 1,2,3,4-tetrahydro-1-naphthol (THNol) on the stabilization of n-tetradecane takes place with the addition of 1 mole%. THNol appears to target secondary radicals to a greater extent than BA at low concentrations of the hydrogen donors.

ACKNOWLEDGMENTS

The authors wish to thank the U.S. Air Force Wright Laboratory, the U.S. DOE / Federal Energy Technology Center for their support. We also thank Prof. Harold H. Schobert for his support and helpful discussion.

REFERENCES

(1) Song, C., Lai, W.-C. and Schobert, H.H., Ind. Eng. Chem. Res., 1994, **33**, 548-557.
(2) Coleman, M.M., Sobkowiak, M., Fearnley, S.P. and Song, C., Prep. Am. Chem. Soc.- Div. Petro. Chem., 1998, **43(3)**, 353-356.
(3) Venkataraman, A., Song, C. and Coleman, M.M., Prep. Am. Chem. Soc.- Div. Petro. Chem., 1998, **43(3)**, 364-367.
(4) Edwards, T., Prep. Am. Chem. Soc.- Div. Petro. Chem., 1996, **41(2)**, 481-487.
(5) Andrésen, J.M., Strohm, J.J. and Song, C., ACS Petroleum Chemistry Division preprints, 43(3), 412-414 (1998).
(6) Song, C., Lai, W.-C. and Schobert, H.H., Ind. Eng. Chem. Res., 1994, **33**, 534-547.

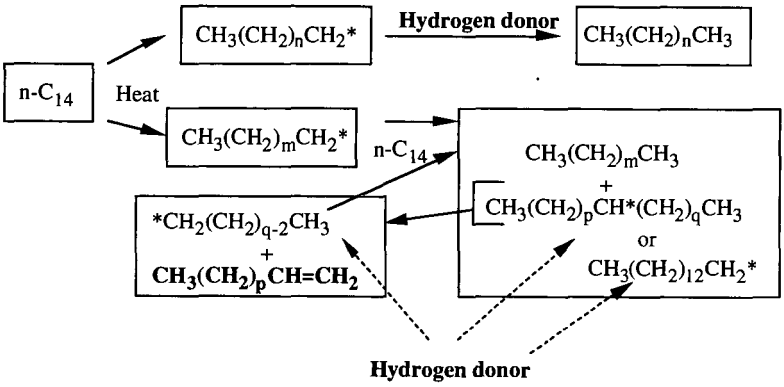

Scheme 1. General concept of the role of the hydrogen donors in stabilizing the n-alkanes leading to suppression of pyrolytic degradation.

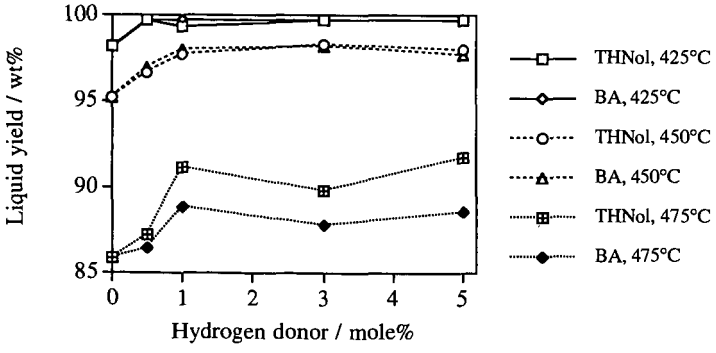

Figure 1. The changes in liquid yields with addition of the hydrogen donors benzyl alcohol and 1,2,3,4-tetrahydro-1-naphthol in the range of 0.5 to 5 mole% at 425, 450 and 475°C.

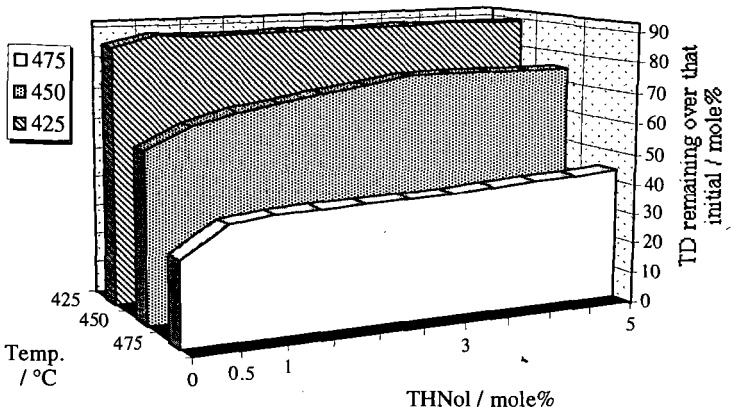

Figure 2. Comparison of remaining n-tetradecane content over its initial concentration for different mixtures with 1,2,3,4-tetrahydro-1-naphthol, stressed at 425, 450 and 475°C for 30 minutes.

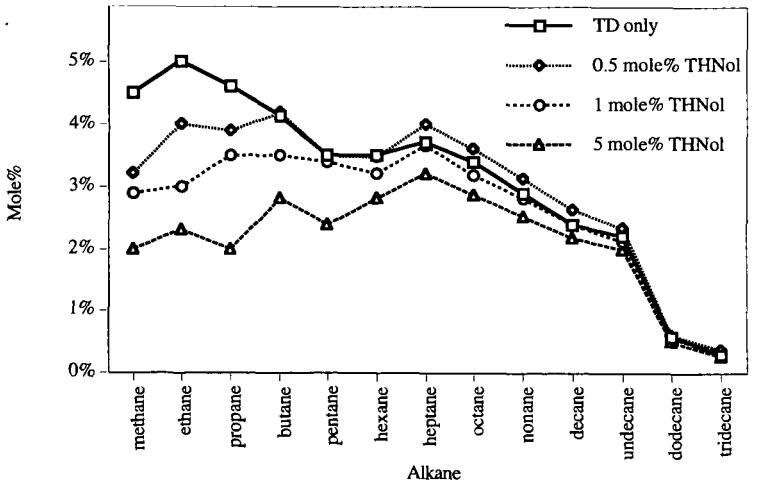

Figure 3. Variation in the n-alkane distribution for pure n-tetradecane and its 0.5, 1 and 5 mole% mixture with 1,2,3,4-tetrahydro-1-naphthol stressed at 450°C for 30 minutes.

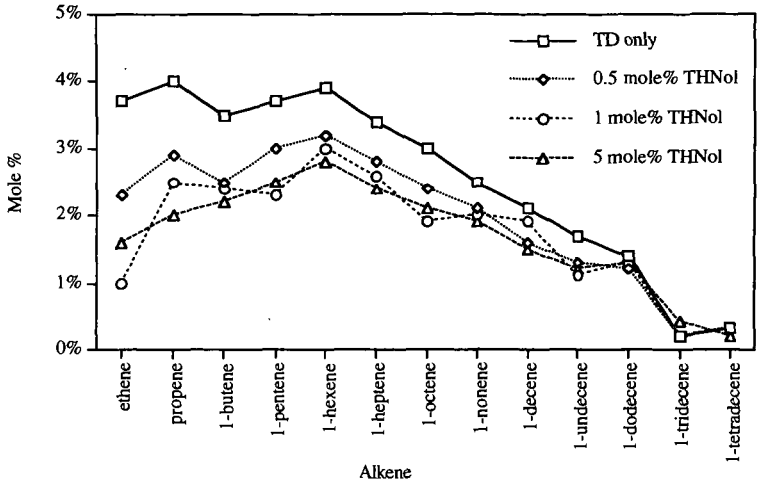

Figure 4. Variation in the 1-alkene distribution for pure n-tetradecane and its 0.5, 1 and 5 mole% mixture with 1,2,3,4-tetrahydro-1-naphthol stressed at 450°C for 30 minutes.

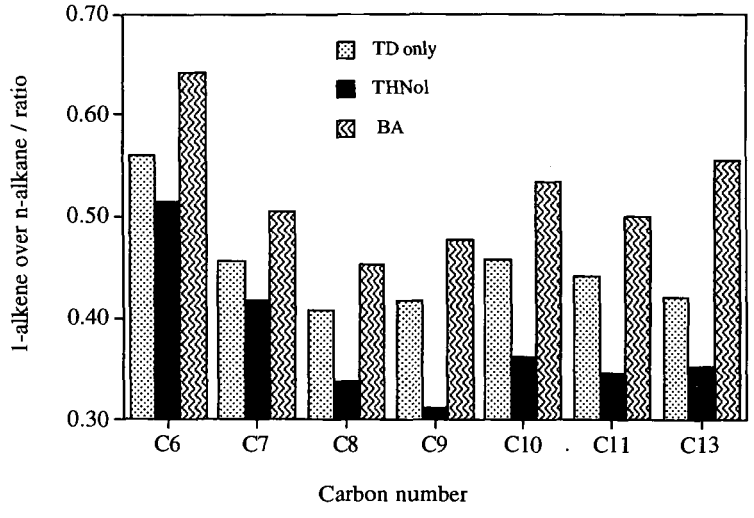

Figure 5. Ratio of the 1-alkene peak area over that of the corresponding alkane for TD alone and with 0.5 mole% THNol and BA addition at 475°C stressed for 30 minutes.

CHEMICAL INTERACTIONS BETWEEN LINEAR AND CYCLIC ALKANES DURING PYROLYTIC DEGRADATION OF JET FUELS

John M. Andrésen, James J. Strohm and Chunshan Song*
Applied Catalysis in Energy Laboratory, The Energy Institute and
Department of Energy and Geo-Environmental Engineering,
The Pennsylvania State University, University Park, PA 16802.

KEYWORDS: Pyrolysis, thermal stability, aviation jet fuels.

ABSTRACT

Potential jet fuels derived from hydrogenation of liquids from coal and petroleum fractions, are rich in both cycloalkanes and long-chain alkanes. Their thermal interactions have been studied using decahydronaphthalene and n-tetradecane as model compounds. Chemical interactions were indicated in the pyrolytic regime by the decrease in gaseous products with increasing addition of decahydronaphthalene to the n-alkane. The improved thermal stability of the n-tetradecane was mainly attributed to the ability of the cycloalkane to capture free radicals from the cracking of the n-alkane.

INTRODUCTION

There is an increasing demand of improved thermal stability of jet fuels for high Mach flights, as illustrated by the JP-900 requirement of the Air Force (1). However, the present aviation jet fuels do not meet these criteria, due to their high content of alkanes in the range C_7-C_{17}, which readily lead to thermal degradation (2). The JP-900 goal has been approached by jet fuels derived from coal liquids (3). Coal derived jet fuels differ substantially from those generally obtained from petroleum in their high content of cyclo-alkanes and a relatively lower concentration of linear alkanes. This chemical distinction is one of the main reasons why coal derived fuels show greater thermal stability in the pyrolytic regime than those of petroleum origin (4). Cyclo-alkanes alone show a great chemical stability in the pyrolytic regime (5). However, due to economical concerns, other potential routes to obtain cyclo-alkane rich fuels are considered, including hydrogenation of aromatic petroleum fractions or by blending of coal and petroleum derived fuels (4). These fuels will still present a relatively high content of long-chain linear alkanes. Earlier tests in batch reactors have shown reduced solid depositions in petroleum fuels at 450°C with addition of decahydronaphthalene (6). This suggests a synergistic effect between the linear and the cyclic alkanes at elevated temperature. Accordingly, this study addresses the chemical interactions between cyclo-alkanes and n-alkanes typical for coal and petroleum derived fuels, where decahydronaphthalene was used as a cyclic model compound, while n-tetradecane represented the linear alkanes.

EXPERIMENTAL

The compounds used were n-tetradecane (TD, Aldrich 99%) and decahydronaphthalene (DHN, Aldrich 98%, a mixture of 46 mole% cis- and 54 mole% trans-decahydronaphthalene). Stressing of TD alone or in 5 or 30 mole% mixtures with DHN were performed for 2 hours in a fludized sandbath at 425, 450 and 475°C. A detailed description of the experimental setup and analytical determination of the product distribution using GC and GC/MS, has been reported elsewhere (4).

RESULTS AND DISCUSSION

Figure 1 compares the gas, liquid and solid yields on a weight basis for pure n-tetradecane (TD) and the mixtures of 5 and 30 mole% decahydronaphthalene (DHN) in TD stressed for 2 hours under an initial pressure of 100 psi N_2 at the

temperatures 425°C (a) and 475°C (b). The development of solids at both temperatures shows the same trend, where the pure TD has a higher value than those observed for both the mixtures. This is especially the case at 475°C, where the pure TD deposited nearly 5 wt% solids compared with around 3 wt% for the mixtures. The liquid residue is in addition lower for the pure TD than for the mixtures (Figure 1). Even at temperatures as low as 425°C, the liquid yield increased from around 82 wt% for TD alone to 97 wt% with only 5 mole% DHN added. Assuming that virtually all the DHN stays in the liquid product (based on evidence discussed later), this corresponds to a relative decrease in the gaseous product from the TD of (18-3.2)/18 = 80%. Similar data was obtained at 450°C. This clearly indicates that DHN prevents gas and solid formation when compared with TD alone. Figure 2 shows that this thermal enhancement is closely related to the reduced cracking of the TD, where the GC traces of the liquid product distribution for TD alone (top) and its mixture with 30 mole% DHN (bottom) stressed at 425°C, are plotted. A great reduction in the cracking products is obtained, where their distribution is shifted towards longer alkanes and 1-alkenes.

Tables 1 to 3 list the total reaction products based on the initial amount at 425, 450 and 475°C for the pure TD and its 5 and 30 mole% DHN mixtures, respectively. With increasing DHN addition, there is a decrease in the amount of linear or branched alkanes at all temperatures, which is also the case for alkenes. The cyclo-alkanes, on the other hand, become more important at higher temperatures, but there is no clear relation to the DHN concentration. Some small amount of alkylated DHN, such as n-butyl-decalin, are also included in these values. In further studies at shorter stressing time (30 minutes), where secondary reactions are expected to be low, a significant amount of ethyl- to dodecyl- substituted decahydronaphthalenes were detected in the liquid products. However, at the relatively long stressing times used here, these intermediates have generally been converted into hydroaromatics (tetralin, alkylated tetralin and indanes) or completely dehydrogenated into naphthalenes (7). However, the increased addition of DHN markedly reduces the development of benzenes, where at 475°C, TD alone produced 23 mole%, while the mixture with 30 mole% DHN only gave 16 mole% benzenes.

The fraction of TD remaining over the initial amount is compared in Figure 3 for the pure TD and its mixtures with 5 and 30 mole% DHN at 425, 450 and 475°C. At 425°C, the increasing content of DHN significantly prevents the thermal decomposition of the TD, where with no DHN added only 40 mole% TD remains compared to nearly 80 mole% for the 30 mole% DHN mixture. Even though this trend is decreasing when the temperature becomes more elevated, there is still a significant rise in the TD content obtained at 450°C with only 5 mole% DHN. After 2 hours stressing at 475°C, the TD has almost vanished and the stabilization effect of the DHN is most likely affecting shorter linear alkanes based on the enhancement in the liquid yield and suppression of solid deposition (Figure 1). Figure 4 compares the remaining DHN over its initial concentration for the 5 and 30 mole% mixtures at 425, 450 and 475°C. Around 90-100 mole% remains up to 450°C followed by a sudden drop at 475°C to around 30-45 mole%. The values are higher for the 5 mole% DHN mixture, as an estimated value of 0.5 % in the calculations gives 0.5/5=10% error in this values (see error bar). The small reduction in DHN concentration at 425 and 450°C is related to stabilization of free radicals via alkylation of the DHN, as discussed earlier. This suggests that DHN at high contents is a benign prohibitor of thermal decomposition of TD up to 450°, due to its own thermal stability.

At increasing temperatures, the benzenes and naphthalenes concentrations are increasing for TD stressed alone and its 5 and 30 mole% DHN mixtures (Tables 1 to 3). The mixtures with DHN are expected to contain a certain amount of naphthalenes due to the dehydrogenation process it experiences during the chemical interaction with the free radical products from the cracking of the TD. Therefore, the total content of naphthalenes must be considered on the basis of the consumed content of DHN. Figure 5 compares the content of naphthalene, where the consumed content of DHN is subtracted, at 450 and 475°C for the pure

TD and its 5 and 30 mole% DHN mixtures. Although resulting in higher overall concentrations of naphthalenes (Tables 1 to 3), Figure 5 illustrates that the naphthalene developed is decreasingly resulting from thermal decomposition of TD as the addition of DHN is increased. This again supports the previous findings that the DHN in mixture with TD prevents thermal decomposition of the n-alkane by suppressing its decomposition into small alkanes and the production of naphthalenes or more condensed aromatic products.

CONCLUSIONS

Tetradecane (TD) has been stressed alone and in mixtures with 5 and 30 mole% decahydronaphthalene (DHN) at 425, 450 and 475°C. A significant decrease in the solid deposition and increase in liquid yields were observed at all temperatures with the addition of DHN. Further, the content of TD remaining was greatly enhanced at temperatures up to 450°C, but was not significant at 475°C due to the thermal decomposition of DHN itself.

ACKNOWLEDGMENTS

The authors wish to thank the U.S. Air Force Wright Laboratory, the U.S. DOE / Federal Energy Technology Center for their support. We also thank Prof. Harold H. Schobert for his support and helpful discussion.

REFERENCES

(1) Edwards, T., Prep. Am. Chem. Soc.-Div. Petro. Chem., 1996, **41(2)**, 481.
(2) Song, C., Lai, W.-C. and Schobert, H.H., Ind. Eng. Chem. Res., 1994, **33**, 534.
(3) Song, C., Eser, S., Schobert, H.H. and Hatcher, P.G., 1993, Energy & Fuels, **7**, 234.
(4) Andrésen, J.M., Strohm, J.J. and Song, C, Prep. Am. Chem. Soc.-Div. Petro. Chem., 1998, **43(3)**, 412.
(5) Lai, W.C. and Song C., Fuel, 1995, **74**, 1436.
(6) Song, C., Lai, W.-C. and Schobert, H.H., Prep. Am. Chem. Soc.-Div. Fuel Chem., 1992, **37(4)**, 1655.
(7) Song, C. and Lai, W.-C., Prep. Am. Chem. Soc.-Div. Petro. Chem., 1998, **43(3)**,462.

Table 1: Distribution of the total reaction products based on the initial amount at 425, 450 and 475°C for the pure TD.

Products / mole%	425°C	450°C	475°C
Alkanes C_{14}^-	22.1	31.6	11.7
Alkanes C_{14}^+	1.8	6.5	<0.1
Cyclo-alkanes	5.1	7.6	7.5
Alkenes	11.7	3.4	1.0
Hydro-aromatics	<0.1	1.8	2.7
Benzenes	<0.1	11.5	23.0
Naphthalene	<0.1	0.9	6.7

Table 2: Distribution of the total reaction products based on the initial amount at 425, 450 and 475°C for the 5 mole% DHN in TD mixture.

Products / mole%	425°C	450°C	475°C
Alkanes C_{14}^-	20.3	27.4	13.1
Alkanes C_{14}^+	7.2	0.6	0.1
Cyclo-alkanes	7.8	8.1	9.5
Alkenes	8.9	1.9	1.3
Hydro-aromatics	<0.1	1.0	3.0
Benzenes	0.1	7.6	21.2
Naphthalene	<0.1	1.8	4.8

Table 3: Distribution of the total reaction products based on the initial amount at 425, 450 and 475°C for the 30 mole% DHN in TD mixture.

Products / mole%	425°C	450°C	475°C
Alkanes C_{14}^-	4.8	15.2	3.6
Alkanes C_{14}^+	1.0	0.5	<0.1
Cyclo-alkanes	3.2	8.0	6.5
Alkenes	2.4	2.2	1.7
Hydro-aromatics	<0.1	3.4	4.4
Benzenes	0.1	7.1	16.0
Naphthalene	<0.1	3.1	14.2

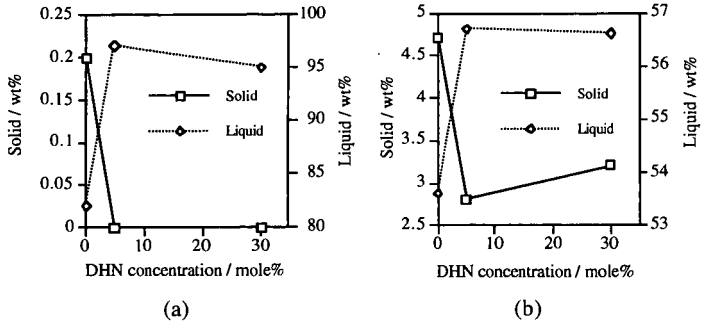

Figure 1. Comparison of liquid and solid yields for pure TD and its mixtures with 5 and 30 mole% DHN stressed for 2 hours under an initial pressure of 100 psi N_2 at the temperatures: (a) 425°C and (b)475°C.

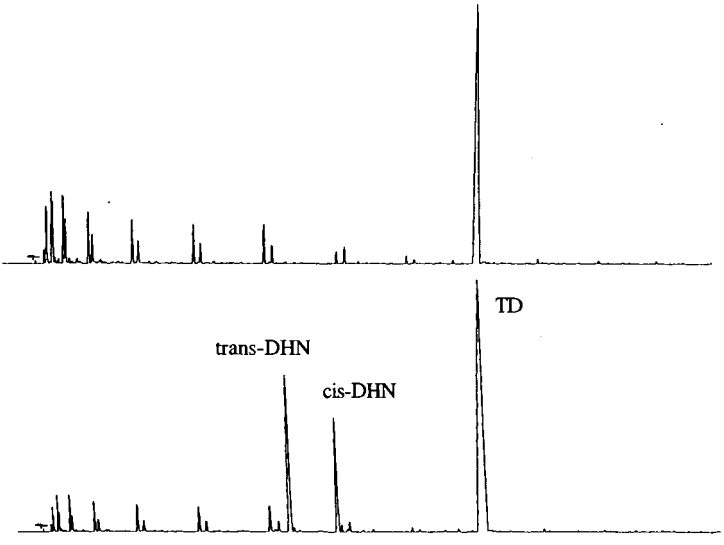

Figure 2. The GC traces of the liquid product distribution for TD alone (top) and its mixture with 30 mole% DHN (bottom) stressed at 425°C.

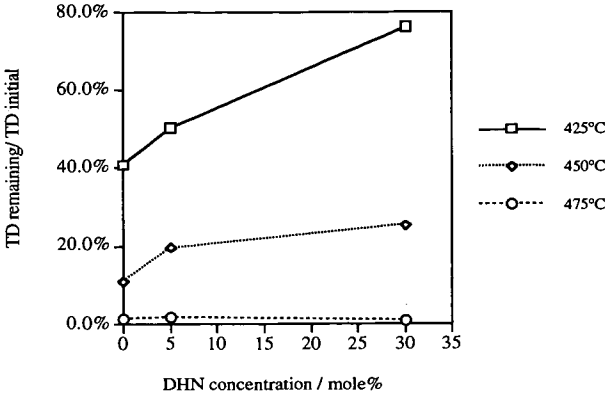

Figure 3. The fraction of TD remaining over its initial concentration for TD alone and its mixtures with 5 and 30 mole% DHN at 425, 450 and 475°C.

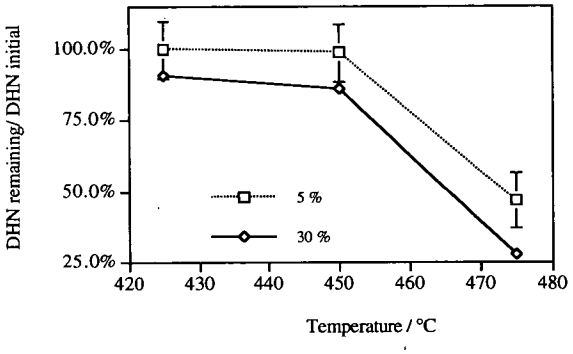

Figure 4. Comparison of the remaining DHN over its initial concentration for the 5 and 30 mole% mixtures with TD at 425, 450 and 475°C.

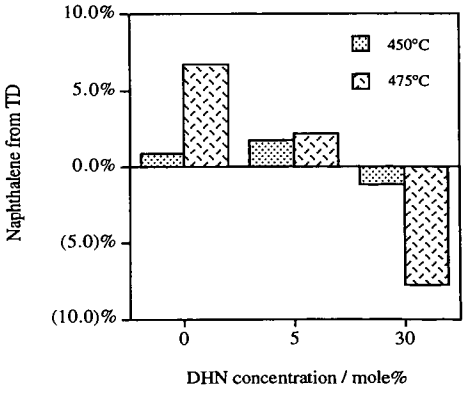

Figure 5. Comparison of the content of naphthalenes where the consumed content of DHN is subtracted at 450 and 475°C for the pure TD and the 5 and 30 mole% DHN in TD mixtures.